Polyaminoquinoline Iron Chelators for Vectorization of Antiproliferative Agents: Design, Synthesis, and Validation

ARTICLE *in* BIOCONJUGATE CHEMISTRY · AUGUST 2012

Impact Factor: 4.51 · DOI: 10.1021/bc300324c · Source: PubMed

13 AUTHORS, INCLUDING:

Emmanuelle Morin-Picardat
University of Eastern Finland
8 PUBLICATIONS **78** CITATIONS
SEE PROFILE

Eric Renault
University of Nantes
62 PUBLICATIONS **507** CITATIONS
SEE PROFILE

Raphaël Tripier
Université de Bretagne Occidentale
87 PUBLICATIONS **837** CITATIONS
SEE PROFILE

David Deniaud
University of Nantes
84 PUBLICATIONS **704** CITATIONS
SEE PROFILE

Bioconjugate Chemistry

Article

pubs.acs.org/bc

Polyaminoquinoline Iron Chelators for Vectorization of Antiproliferative Agents: Design, Synthesis, and Validation

Vincent Corcé,[†,‡] Emmanuelle Morin,[†] Solène Guihéneuf,[†] Eric Renault,[†] Stéphanie Renaud,[‡] Isabelle Cannie,[‡] Raphaël Tripier,[§] Luís M. P. Lima,[§] Karine Julienne,[†] Sébastien G. Gouin,[†] Olivier Loréal,[‡] David Deniaud,*[,†] and François Gaboriau*[,‡]

[†]LUNAM Université, CEISAM, Chimie Et Interdisciplinarité, Synthèse, Analyse, Modélisation, UMR CNRS 6230, UFR des Sciences et des Techniques, 2, rue de la Houssinière, BP 92208, 44322 NANTES Cedex 3, France

[‡]INSERM, UMR991, CHRU Pontchaillou, 35033 Rennes, France; Université de Rennes1, 35043 Rennes, France

[§]CNRS, UMR 6521, Université de Brest, Laboratoire de Chimie, Electrochimie Moléculaires et Chimie Analytique, 6 Avenue Victor Le Gorgeu, 29200 Brest, France

S *Supporting Information*

ABSTRACT: Iron chelation in tumoral cells has been reported as potentially useful during antitumoral treatment. Our aim was to develop new polyaminoquinoline iron chelators targeting tumoral cells. For this purpose, we designed, synthesized, and evaluated the biological activity of a new generation of iron chelators, which we named Quilamines, based on an 8-hydroxyquinoline (8-HQ) scaffold linked to linear polyamine vectors. These were designed to target tumor cells expressing an overactive polyamine transport system (PTS). A set of Quilamines bearing variable polyamine chains was designed and assessed for their ability to interact with iron. Quilamines were also screened for their cytostatic/cytotoxic effects and their selective uptake by the PTS in the CHO cell line. Our results show that both the 8-HQ moiety and the polyamine part participate in the iron coordination. **HQ1−44**, the most promising Quilamine identified, presents a homospermidine moiety and was shown to be highly taken up by the PTS and to display an efficient antiproliferative activity that occurred in the micromolar range. In addition, cytotoxicity was only observed at concentrations higher than 100 μM. We also demonstrated the high complexation capacity of **HQ1−44** with iron while much weaker complexes were formed with other cations, indicative of a high selectivity. We applied the density functional theory to study the binding energy and the electronic structure of prototypical iron(III)-Quilamine complexes. On the basis of these calculations, Quilamine **HQ1−44** is a strong tridentate ligand for iron(III) especially in the form of a 1:2 complex.

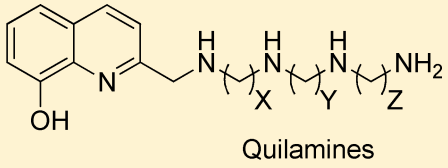

Quilamines

INTRODUCTION

Iron is an essential metal in many biological functions and an interesting and innovative target for anticancer therapy.[1] Growing tumor cells require large quantities of iron, expressed by an increase in the import proteins and a decrease in the export proteins of iron.[2,3] The activity and expression of ribonucleotide reductase (RR), the iron-dependent key enzyme regulating DNA synthesis and cell proliferation, are increased in tumor cells.[4] Previous studies have reported the relationship between body iron stores and the risk of cancers.[5,6] The iron load stimulates the proliferation of tumor cells *in vitro* and *in vivo*.[7] The need for iron during the cell cycle is illustrated by the overexpression of proliferating transferrin receptor cells on the plasma membrane, which allows transferrin-chelated iron to enter the cell.[8] In contrast, the underexpression of the cellular iron exporter, ferroportin, leads to an intracellular accumulation of iron, and is a biomarker for tumor growth in breast cancer.[9,10] Decreasing the exchangeable intracellular iron level with synthetic metal chelators is therefore an attractive method for limiting the proliferation of cancer cells.[11]

Iron chelators, like Deferoxamine initially developed for the treatment of primary iron overload, as well as Deferiprone[12,13] and Deferasirox,[14] more recently developed for the treatment of secondary overloads (thalassemias), inhibit the proliferation of tumor cells in culture. Their antiproliferative effects are modulated by their iron-chelating capacity and their cellular uptake. We recently showed that the antiproliferative effect of ICL670, a tridentate iron chelator with a hydroxyphenyltriazole skeleton (Deferasirox, Novartis Pharma), and O-Trensox resulted from the iron depletion induced in cells and the inhibitory action on the polyamine metabolism.[15,16] Deferoxamine inhibits the growth of melanoma and hepatoma cells *in vitro* and *in vivo*.[17] This chelator was effective in the treatment of leukemias and neuroblastomas in preliminary clinical trials.[18] The high antiproliferative activity observed with iron chelators derived from pyridoxal isonicotinoyl hydrazone, including aroylhydrazones and thiosemicarbazones, was assumed to involve both their iron-chelating efficiency and their ability to generate reactive oxygen species.[1] More recently, iron depletion induced by the iron chelators Deferoxamine and 2-hydroxyl-1-

Received: June 19, 2012
Revised: July 24, 2012
Published: August 8, 2012

dx.doi.org/10.1021/bc300324c | *Bioconjugate Chem.* 2012, 23, 1952−1968

naphtylaldehyde isonicotinoyl hydrazone was shown to increase the expression of growth arrest and DNA damage genes.[19]

All these results suggest that, due to their antiproliferative and apoptotic properties, iron chelators could be used as an adjuvant in the treatment of cancers. The mechanism of action of cytotoxic antitumor agents, like Doxorubicin and Bleomycin, involves their iron-chelating ability to some extent. However, such therapy must target tumoral cells. In fact, conversely to what is observed in iron overload diseases, cells are not overloaded and the iron stores are not excessive. Therefore, uncontrolled iron depletion of normal cells may generate strong adverse effects. Despite the fact that tumoral cells require more iron, an antiproliferative therapeutic strategy based on iron deprivation of tumoral cells will benefit from a specific vectorization of the iron chelators to these cells.

Polyamine metabolism (biosynthesis and uptake), detrimental to cell proliferation, is also particularly amplified in tumor cells.[20] The Polyamine Transport System (PTS), which can deal with natural and synthetic polyamines, is increased in tumor cells.[21] This property is of potential interest to target antitumor agents.[22−24] Thus, various polyamine analogues have been grafted onto cytotoxic compounds like nitroimidazole,[25] chlorambucil,[26] acridine,[27] anthracene,[28] camptothecine,[29] naphthoquinone,[30] azepine, and benzazepine.[31] This concept of tumor vectorization by polyamines has also been developed to inhibit their own transporter,[32,33] to vectorize cytotoxic compounds such as dimethylsilane polyamine derivatives[34] or molecules carrying boron atoms for boronotherapy,[35,36] and finally to monitor the intracellular traffic of polyamines toward the cells by using fluorescent polyamine analogues.[28,37−39] More recently, F14512, a novel spermine epipodophyllotoxin conjugate, and inhibitor of DNA-topoisomerase II,[40] was selected for clinical development in AML phase I.

In order to generate iron chelator molecules targeting tumor cells, we planned to associate polyamine cargos with iron-chelating units to promote the uptake of the chelating motif by the overactive polyamine transport system of tumor cells.

For this purpose, we synthesized and evaluated a new generation of chelator-polyamine hybrids (Quilamines) which were designed to decrease the iron content in the iron complexes in cancerous cells, thus reducing tumor cell proliferation. The difference in PTS activation between healthy cells and tumor cells enables tumor cells to be targeted, whereas the strong dependence of these cells on iron ensures a secondary targeting.

Such a concept has been reported in previous studies on the synthesis and the biological properties of a chelating Deferiprone-type moiety linked to spermine.[41] In addition, other studies revealed that homospermidine−anthracene conjugates were more selectively recognized by the PTS than spermine derivatives.[38] Instead, we chose the hydroxyquinoline moiety, found in the iron chelator O-Trensox, which has a higher affinity for iron than Deferiprone.[42] The potential value of this structure in an anticancer strategy is illustrated by the example of Clioquinol (5-chloro-7-iodo-8-hydroxyquinoline). This antibiotic is also able to chelate metals, which results in an antiproliferative activity on tumor cells in culture and on grafted tumors in animals.[43,44] The structural requirement of the PTS for polyamine analogues has previously been demonstrated, showing its selectivity for a single CH_2 spacer between the heterocyclic part linked to a homospermidine moiety.[39,45]

In order to meet these objectives, we report here the synthesis of the first generation of Quilamines: a hydroxyquinoline moiety (HQ) linked by a single carbon atom (HQ1) to a linear polyamine chain of various types including the spermidine (HQ1-*XY*) and spermine (HQ1-*XYZ*) series (*X*, *Y*, and *Z* represent the alkyl chain length between the amino groups). In a cellular model, we screened the antiproliferative efficiency of these polyaminoquinolines (Quilamines) HQ1-*XYZ* as well as their specificity for the polyamine transport system. Finally, we evaluated the complexation properties of the most biologically efficient Quilamine **HQ1−44** toward iron(III) and competitive cations.

EXPERIMENTAL PROCEDURES

Chemistry. NMR spectra were recorded at room temperature with a Bruker Avance 300 Ultra Shield or Bruker Avance III 400 spectrometers. Chemical shifts are reported in parts per million (ppm); coupling constant are reported in units of Hertz [Hz]. Infrared (IR) spectra were recorded with a Bruker Vector 22 FTIR using KBr films or KBr pellets. Low-resolution mass spectra (MS) were recorded with a Thermo electron DSQ spectrometer. High-resolution mass spectra (HRMS) were recorded with a Thermofisher hybrid LTQ-orbitrap spectrometer (ESI^+) and with a Bruker Autoflex III SmartBeam spectrometer (MALDI). Microanalyses were performed on a Thermo Scientific FLASH 2000 Series CHNS/O Analyzers. Melting points were determined in open capillary tubes and are uncorrected. All reagents were purchased from Acros Organics or Aldrich and were used without further purification. Column chromatographies were conducted on silica gel Kieselgel SI60 (40−63 μm) from Merck. Reactions requiring anhydrous conditions were performed under argon. Dichloromethane was distilled from calcium hydride under nitrogen prior to use. Toluene and tetrahydrofuran were distilled from sodium/benzophenone under argon prior to use.

The compounds **1**−**5**, **8**−**20**, **24**, **25**, **28**, and **29** already have been described in the literature.

*Compound (**21**).* To solution of N^1,N^4-di-*tert*-butyloxycarbonylspermidine **3** (1 g, 2.9 mmol) in anhydrous acetonitrile (30 mL) was added potassium carbonate (1.41 g, 10.15 mmol), and the suspension was stirred at room temperature for 10 min under Ar. 4-Bromobutyronitrile (290 μL, 2.9 mmol) was added, and the resulting mixture was then stirred for 20 h at 50 °C. The mixture was filtered, the solvent was removed under reduced pressure, and the residue was purified by chromatography on silica gel ($CHCl_3$/MeOH/NH_4OH, 94:5:1) to give compound **21** as a colorless oil (850 mg, 71%).

*Compound (**21**).* Colorless oil (850 mg, 71%). IR (KBr): ν = 3349, 2974, 2932, 2866, 1693, 1515, 1478, 1454, 1418, 1390, 1365, 1273, 1250, 1168, 868, 774 cm^{-1}. ^1H NMR (400 MHz, [D_4]MeOD): δ = 1.39−1.64 (m, 22H, 2CH_2 3CH_3), 1.69 (q, 2H, CH_2, J = 7 Hz), 1.82 (q, 2H, CH_2, J = 7.24 Hz), 2.51 (t, 2H, CH_2, J = 7.16 Hz), 2.61 (dd, 2H, CH_2, J = 7.14 Hz, J = 7.44 Hz), 2.69 (dd, 2H, CH_2, J = 7.14 Hz, J = 7.44 Hz), 3.03 (t, 2H, CH_2, J = 6.78 Hz), 3.17−3.26 (m, 4H, 2CH_2) ppm. ^{13}C NMR (100 MHz, [D_4]MeOD): δ = 15.3, 26.3, 26.9, 27.7, 28.7 (tBu), 28.8 (tBu), 30.2, 38.9, 45.6, 48.1, 49.1, 50.3, 79.9, 80.9, 120.9, 137.5, 158.4. HRMS (MALDI): calcd. for $C_{21}H_{40}N_4O_4$ [M+H]$^+$ 413.3122; found 413.3118.

*General Procedure for the Preparation of Cyanopolyamines **22** and **23**.* To solution of di-*tert*-butyloxycarbonylhomospermidine **1** (0.2 g, 1.06 mmol) for **22** or di-*tert*-butyloxycarbonylspermidine **3** (0.2 g, 1.06 mmol) for **23** in methanol was added acrylonitrile (70.3 μL, 1.06 mmol) under Ar at 0 °C and stirred for 6 h, and the reaction mixture was

stirred at room temperature over a period of 12 h. The solvent was removed under reduced pressure and the residue was purified by chromatography on silica gel (chloroform/methanol/ammonia, 94:5:1).

*Compound (**22**).* Colorless oil (730 mg, 91%). IR (KBr): ν = 3347, 2974, 2932, 2863, 1688, 1521, 1478, 1454, 1418, 1390, 1365, 1251, 1171 cm^{-1}. ^1H NMR (400 MHz, [D_4]MeOD): δ = 1.43 (s, 9H, tBu), 1.46 (s, 9H, tBu), 1.46−1.63 (m, 8H, 4CH_2), 2.60 (t, 2H, CH_2, J = 6.85 Hz), 2.63 (dd, 2H, CH_2, J = 7.1 Hz), 2.87 (dd, 2H, CH_2, J = 6.76 Hz), 3.05 (t, 2H, CH_2, J = 6.8 Hz), 3.17−3.26 (m, 4H, 2CH_2) ppm. ^{13}C NMR (100 MHz, [D_4]MeOD): δ = 18.3, 26.5, 26.9, 27.8, 28.3, 28.7 (6C), 41.0, 45.9, 47.9 (2C), 49.7, 79.8, 80.8, 119.9, 157.4, 158.5. HRMS (MALDI): calcd. for $C_{21}H_{40}N_4O_4$ [M+Na]$^+$ 435.2942; found 435.2942.

*Compound (**23**).* Colorless oil (83%). IR (KBr): ν = 3582, 3341, 2976, 2932, 2863, 1683, 1520, 1479, 1418, 1390, 1365, 1251, 1164, 1081, 1040, 993, 869, 775 cm^{-1}. ^1H NMR (400 MHz, [D_4]MeOD): δ = 1.43 (s, 9H, 3CH_3), 1.46 (s, 9H, 3CH_3), 1.47−1.63 (m, 4H, 2CH_2), 1.69 (q, 2H, CH_2, J = 7 Hz), 2.60 (t, 2H, CH_2, J = 6.8 Hz), 2.63 (dd, 2H, CH_2, J = 7.1 Hz, J = 7.3 Hz), 2.86 (t, 2H, CH_2, J = 6.9 Hz), 3.03 (t, 2H, CH_2, J = 6.8 Hz), 3.17−3.27 (m, 4H, 2CH_2) ppm. ^{13}C NMR (100 MHz, [D_4]MeOD): δ = 18.3, 26.9, 27.8, 28.3, 28.7 (3C), 28.8 (3C), 41.0, 45.9, 47.9 (2C), 49.7, 79.9, 80.9, 119.9, 157.4, 158.4. HRMS (MALDI): calcd. for $C_{20}H_{38}N_4O_4$ [M+Na]$^+$ 421.2785; found 421.2774.

*General Procedure for the Preparation of Cyanopolyamines **26** and **27**.* A solution of di-*tert*-butyldicarbonate (2.5 equiv, 3.3 mmol) in anhydrous methanol was added dropwise to a stirring solution of **21** (1 equiv, 1.32 mmol) or **22** (1 equiv, 1.32 mmol) in solution of methanol and 10% of triethylamine (10 mL). After stirring for 24 h at room temperature, solvents were removed under reduced pressure to give a colorless oil, which was dissolved in dichloromethane, washed with saturated $NaHCO_3$ and then water. The organic layer was separated, dried over anhydrous Na_2SO_4, filtered, and concentrated under reduced pressure. The residue was purified by chromatography on silica gel (dichloromethane then dichloromethane/ethyl acetate: (8:2)).

*Compound (**26**).* Colorless oil (670 mg, 98%). IR (KBr): ν = 3360, 2975, 2932, 2868, 1698, 1519, 1479, 1455, 1417, 1390, 1366, 1249, 1163, 1077, 1040, 872, 773 cm^{-1}. ^1H NMR (400 MHz, [D_4]MeOD): δ = 1.43 (s, 9H, 3CH_3), 1.46 (s, 9H, 3CH_3), 1.47 (s, 9H, 3CH_3), 1.49−1.58 (m, 4H, 2CH_2), 1.69 (q, 2H, CH_2, J = 6.9 Hz), 1.87 (q, 2H, CH_2, J = 7 Hz), 2.44 (t, 2H, CH_2, J = 7 Hz), 3.03 (t, 2H, CH_2, J = 6.8 Hz), 3.17−3.27 (m, 6H, 3CH_2), 3.32 (t, 2H, CH_2, J = 7.1 Hz) ppm. ^{13}C NMR (100 MHz, [D_4]MeOD): δ = 14.9, 25.6, 26.6, 27.0, 28.75 (3C), 28.78 (3C), 28.8 (3C), 29.5, 30.3, 38.9, 45.9, 47.1, 47.8 (2C), 79.9, 80.9, 81.3, 120.8, 157.4, 158.4. HRMS (MALDI): calcd. for $C_{26}H_{48}N_4O_6$ [M+Na]$^+$ 535.3466; found 535.3463.

*Compound (**27**).* Colorless oil (395 mg, 99%). IR (KBr): ν = 3360, 2975, 2932, 2867, 1682, 1519, 1479, 1417, 1391, 1366, 1251, 1163, 1074, 871, 774 cm^{-1}. ^1H NMR (400 MHz, [D_4]MeOD): δ = 1.43 (s, 9H, 3CH_3), 1.46 (s, 9H, 3CH_3), 1.48 (s, 9H, 3CH_3), 1.50−1.61 (m, 8H, 4CH_2), 2.69 (t, 2H, CH_2, J = 6.6 Hz), 3.05 (t, 2H, CH_2, J = 6.8 Hz), 3.16−3.26 (m, 4H, 2CH_2), 3.29 (t, 2H, CH_2, J = 6.6 Hz), 3.50 (t, 2H, CH_2, J = 6.6 Hz) ppm. ^{13}C NMR (100 MHz, [D_4]MeOD): δ = 17.3 and 17.8 (rotamer), 26.8 (4C), 28.3 (3C), 28.6 (3C), 28.8 (3C), 41.0, 44.3, and 44.6 (rotamer), 48.1 (3C), 79.8, 80.8, 81.7, 119.5, 157.1, 157.4, 158.5. HRMS (MALDI): calcd. for $C_{26}H_{48}N_4O_6$ [M+Na]$^+$ 535.3466; found 535.3479.

*General Procedure for the Preparation of Homospermines **6** and **7**.* To a suspension of Raney Ni (2 g) in ethanol (10 mL) was added cyanopolyamines **26** or **27** (1 equiv, 1.4 mmol) and slowly NH_4OH (4 mL). The mixture was stirred under hydrogen (20 bar) at room temperature for 24 h. The Raney nickel was eliminated by filtration over a pad of Celite, and the filtrate was evaporated under reduce pressure. The resulting solid was dissolved in dichloromethane, washed with NaOH 2.5 M (2 times) and water, dried over anhydrous Na_2SO_4, filtered, and concentrated under reduced pressure to yield homospermine **6** or **7** as a colorless oil.

*Compound (**6**).* Colorless oil (99%). IR (KBr): ν = 3363, 2973, 2930, 2865, 1689, 1520, 1479, 1418, 1390, 1365, 1275, 1250, 1169, 875, 773 cm^{-1}. ^1H NMR (400 MHz, [D_4]MeOD): δ = 1.43 (s, 9H, 3CH_3), 1.45 (s, 9H, 3CH_3), 1.46 (s, 9H, 3CH_3), 1.48−1.63 (m, 8H, 4CH_2), 1.68 (q, 2H, CH_2, J = 6.8 Hz), 2.64 (dd, 2H, CH_2, J = 7.1 Hz), 3.03 (t, 2H, CH_2, J = 6.8 Hz), 3.16−3.27 (m, 8H, 4CH_2) ppm. ^{13}C NMR (100 MHz, [D_4]MeOD): δ = 26.7, 27.1, 28.8 (9C), 29.6, 30.2, 31.1, 38.9, 42.3, 48.1 (4C), 79.9, 80.8, 80.9, 157.4 (2C), 158.4. HRMS (MALDI): calcd. for $C_{26}H_{52}N_4O_6$ [M+Na]$^+$ 539.3779; found 539.3760.

*Compound (**7**).* Colorless oil (99%). IR (KBr): ν = 3362, 2974, 2931, 2866, 1683, 1520, 1479, 1455, 1418, 1390, 1365, 1251, 1170, 875, 773 cm^{-1}. ^1H NMR (400 MHz, [D_4]MeOD): δ = 1.43 (s, 9H, 3CH_3), 1.45 (s, 9H, 3CH_3), 1.46 (s, 9H, 3CH_3), 1.48−1.61 (m, 8H, 4CH_2), 1.68 (q, 2H, CH_2, J = 6.9 Hz), 2.62 (t, 2H, CH_2, J = 6.9 Hz), 3.04 (t, 2H, CH_2, J = 6.8 Hz), 3.15−3.29 (m, 8H, 4CH_2) ppm. ^{13}C NMR (100 MHz, [D_4]MeOD): δ = 26.5 (2C), 27.1 (2C), 28.3 (3C), 28.8 (6C), 32.1, 39.6, and 40.0 (rotamer), 41.0, 45.1, and 45.8 (rotamer), 47.9 (3C), 79.8, 80.8, 80.9, 157.4 (2C), 158.5. HRMS (MALDI): calcd. for $C_{26}H_{52}N_4O_6$ [M+Na]$^+$ 539.3779; found 539.3781.

*General Procedure for the Reductive Amination (**31**−**39**).* To a stirred solution of polyamines **1**−**9** (1.2 equiv, 0.72 mmol) in 1,2-dichloroethane (6 mL) at room temperature under argon was added 8-hydroxyquinoline-2-carbaldehyde **30** (1 equiv, 0.6 mmol). After 15 min, sodium triacetoxyborohydride (3 equiv, 1.8 mmol) was added and the mixture was stirred 2 to 4 h until aldehyde was consumed (monitored by TLC). The reaction mixture was quenched by adding 1 M NaOH, stirred 20 min, and the product was extracted three times with CH_2Cl_2, dried over anhydrous Na_2SO_4, filtered, and concentrated under reduced pressure. The residue was purified by chromatography on silica gel (chloroform/methanol/ammonia, 94:5:1 for **31**−**34**; and 95:4:1 for **35**−**39**).

*Compound (**31**).* Viscous yellow oil (705 mg, 91%). IR (KBr): ν = 3053, 2982, 2934, 1706, 1683, 1575, 1507, 1475, 1455, 1420, 1391, 1366, 1265, 1168, 1047 cm^{-1}. ^1H NMR (400 MHz, [D_4]MeOD): δ = 1.35−1.69 (m, 26H, 8CH_2 6CH_3), 2.77 (bs, 2H, CH_2), 3.03 (t, 2H, CH_2, J = 6.8 Hz), 3.13−3.26 (m, 4H, 2CH_2), 4.14 (s, 2H, CH_2), 7.10 (dd, H, J = 7.5 Hz, J = 1.3 Hz), 7.34 (dd, H, J = 8.3 Hz, J = 1.3 Hz), 7.41 (dd, H, J = 8.1 Hz, J = 7.6 Hz), 7.45 (d, H, J = 8.5 Hz), 8.20 (d, H, J = 8.5 Hz) ppm. ^{13}C NMR (100 MHz, [D_4]MeOD): δ = 26.5, 27.0, 27.2, 28.4, 28.7 (3C), 28.8 (3C), 40.9, 48.1, 49.9, 54.9, 79.8, 80.8, 112.2, 118.8, 122.1, 128.3, 129.4, 137.9, 139.2, 154.2, 157.4 (2C), 158.5. HRMS (MALDI): calcd. for $C_{28}H_{44}N_4O_5$ [M+H]$^+$ 517.3384; found 517.3386.

*Compound (**32**).* Viscous yellow oil (300 mg, 82%). IR (KBr): ν = 3341, 2974, 2933, 2824, 1689, 1595, 1573, 1508, 1476, 1420, 1391, 1366, 1274, 1230, 1169, 1088, 1034 cm^{-1}. ^1H NMR (400 MHz, [D_4]MeOD): δ = 1.36−1.48 (m, 18H, 9CH_3), 1.54−1.61 (m, 4H, 2CH_2), 1.66 (qt, 2H, CH_2, J = 6.8 Hz), 2.71 (t, 2H, CH_2, J = 6.8 Hz), 3.02 (t, 2H, CH_2, J = 6.8 Hz), 3.14−3.26 (m, 4H, 2CH_2), 4.07 (s, 2H, CH_2), 7.09 (dd, H, J = 7.5 Hz, J = 1.3 Hz), 7.32 (dd, H, J = 8.3 Hz, J = 1.3 Hz), 7.38 (dd, H, J = 7.6 Hz, J = 7.5 Hz), 7.42 (d, H, J = 8.5 Hz), 8.17 (d, H, J = 8.5 Hz) ppm. ^{13}C NMR (100 MHz, [D_4]MeOD): δ = 27.5 (2C), 28.7 (3C), 28.8 (3C), 29.4 and 30.2 (rotamer), 38.9, 45.6, and 46.1 (rotamer), 48.1, 50.1, 55.3, 79.9, 80.9, 112.1, 118.8, 122.1, 128.2, 129.4, 137.8, 139.3, 154.2, 157.4, 158.2, 158.4. HRMS (MALDI): calcd. for $C_{27}H_{42}N_4O_5$ $[M+H]^+$ 503.3228; found 503.3207.

*Compound (**33**).* Viscous yellow oil (280 mg, 90%). IR (KBr): ν = 3350.4, 2975, 2935, 2826, 1688, 1575−1250, 1171, 1033 cm^{-1}. ^1H NMR (400 MHz, [D_4]MeOD): δ = 1.32−1.61 (m, 22H, 2CH_2 6CH_3), 1.83 (qt, 2H, CH_2, J = 7.1 Hz), 2.72 (bt, 2H, CH_2), 3.03 (t, 2H, CH_2, J = 6.8 Hz), 3.17 (t, 2H, CH_2, J = 7.2 Hz), 3.22−3.38 (m, 2H, CH_2), 4.09 (s, 2H, CH_2), 7.10 (dd, H, J = 7.5 Hz, J = 1.3 Hz), 7.33 (dd, H, J = 8.3 Hz, J = 1.3 Hz), 7.39 (dd, H, J = 8.3 Hz, J = 7.6 Hz), 7.43 (d, H, J = 8.5 Hz), 8.18 (d, H, J = 8.5 Hz) ppm. ^{13}C NMR (100 MHz, [D_4]MeOD): δ = 26.9, 28.3, 28.7 (3C), 28.8 (3C), 29.6, 40.9, 45.3, 46.4, and 46.9 (rotamer), 47.8, 54.8, 79.8, 80.9, 112.1, 118.8, 122.1, 128.3, 129.4, 137.9, 139.2, 154.2, 157.5, 158.5 (2C). HRMS (MALDI): calcd. for $C_{27}H_{42}N_4O_5$ $[M+H]^+$ 503.3228; found 503.3215.

*Compound (**34**).* Viscous yellow oil (325 mg, 88%). IR (KBr): ν = 3357, 2976, 2935, 2827, 1689, 1600, 1574, 1509, 1477, 1422, 1392, 1367, 1251, 1170, 1089, 1033 cm^{-1}. ^1H NMR (400 MHz, [D_4]MeOD): δ = 1.42 (s, 18H, 6CH_3), 1.68 (qt, 2H, CH_2, J = 6.3 Hz), 1.83 (qt, 2H, CH_2, J = 7.1 Hz), 2.69 (t, 2H, CH_2, J = 7 Hz), 3.02 (t, 2H, CH_2, J = 6.8 Hz), 3.21 (t, 2H, CH_2, J = 7.2 Hz), 3.25−3.38 (m, 2H, CH_2), 4.08 (s, 2H, CH_2), 7.09 (dd, H, J = 7.5 Hz, J = 1.3 Hz), 7.33 (dd, H, J = 8.2 Hz, J = 1.2 Hz), 7.39 (dd, H, J = 8.1 Hz, J = 7.6 Hz), 7.44 (d, H, J = 8.5 Hz), 8.18 (d, H, J = 8.5 Hz) ppm. ^{13}C NMR (100 MHz, [D_4]MeOD): δ = 28.7 (3C), 28.8 (3C), 29.5, 30.1, 38.9, 45.8, 46.5, 49.8, 55.1, 79.9, 81.1, 112.1, 118.8, 122.1, 128.3, 129.4, 137.8, 139.2, 154.2, 157.5, 158.4 (2C). HRMS (MALDI): calcd. for $C_{26}H_{40}N_4O_5$ $[M+H]^+$ 489.3071; found 489.3048.

*Compound (**35**).* Viscous yellow oil (200 mg, 95%). IR (KBr): ν = 3351, 2974, 2932, 2865, 1699, 1601, 1573, 1506, 1472, 1418, 1366, 1250, 1173, 879, 836, 754 cm^{-1}. ^1H NMR (400 MHz, [D_4]MeOD): δ = 1.39−1.65 (m, 35H, 4CH_2 9CH_3), 2.72 (bt, 2H, CH_2), 3.03 (t, 2H, CH_2, J = 6.7 Hz), 3.13−3.24 (m, 8H, 4CH_2), 4.09 (s, 2H, CH_2), 7.09 (dd, H, J = 7.5 Hz, J = 1.3 Hz), 7.33 (dd, H, J = 8.2 Hz, J = 1.3 Hz), 7.39 (dd, H, J = 8.2 Hz, J = 7.5 Hz), 7.44 (d, H, J = 8.5 Hz), 8.19 (d, H, J = 8.5 Hz) ppm. ^{13}C NMR (100 MHz, [D_4]MeOD): δ = 26.6 (2C), 27.1 (2C), 27.6, 28.3, 28.8 (9C), 41.0, 48.0 (4C), 50.1, 55.3, 79.8, 80.8 (2C), 112.1, 118.8, 122.2, 128.3, 129.4, 137.8, 139.3, 154.2, 157.4 (2C), 158.2, 158.5. HRMS (MALDI): calcd. for $C_{37}H_{61}N_5O_7$ $[M+H]^+$ 688.4644; found 688.4672.

*Compound (**36**).* Viscous yellow oil (310 mg, 94%). IR (KBr): ν = 3360, 3051, 2972, 2929, 2864, 1695, 1616, 1558, 1520, 1506, 1495, 1472, 1464, 1456, 1363, 1248, 1164, 1090, 1044, 1005, 877, 835 cm^{-1}. ^1H NMR (400 MHz, [D_4]MeOD): δ = 1.34−1.61 (m, 35H, 4CH_2 9CH_3), 1.83 (qt, 2H, CH_2, J = 7.1 Hz), 2.70 (t, 2H, CH_2, J = 6.9 Hz), 3.04 (t, 2H, CH_2, J = 6.8 Hz), 3.13−3.25 (m, 6H, 3CH_2), 3.31 (m, 2H, CH_2), 4.08 (s, 2H, CH_2), 7.09 (dd, H, J = 7.4 Hz, J = 1.35 Hz), 7.34 (dd, H, J = 8.2 Hz, J = 1.35 Hz), 7.40 (dd, H, J = 8.2 Hz, J = 7.4 Hz), 7.45 (d, H, J = 8.5 Hz), 8.19 (d, H, J = 8.5 Hz) ppm. ^{13}C NMR (100 MHz, [D_4]MeOD): δ = 26.6 (2C), 27.0 (2C), 28.3, 28.7 (3C), 28.8 (6C), 41.0, 47.9 (4C), 49.8, 55.1, 79.8, 80.8, 80.9, 112.0, 118.8, 122.1, 128.3, 129.4, 137.8, 139.3, 154.2, 157.4 (2C), 157.5, 158.5. HRMS (MALDI): calcd. for $C_{36}H_{59}N_5O_7$ $[M+H]^+$ 674.4487; found 674.4492.

*Compound (**37**).* Viscous yellow oil (485 mg, 96%). IR (KBr): ν = 3357, 3052, 2975, 2931, 1683, 1600, 1573, 1505, 1471, 1418, 1390, 1366, 1248, 1164, 1086, 878, 835, 754, 703 cm^{-1}. ^1H NMR (400 MHz, [D_4]MeOD): δ = 1.35−1.53 (m, 33H, 3CH_2 9CH_3), 1.53−1.62 (m, 4H, 2CH_2), 2.70 (bt, 2H, CH_2), 3.02 (t, 2H, CH_2, J = 6.7 Hz), 3.21−3.26 (m, 8H, 4CH_2), 4.07 (s, 2H, CH_2), 7.08 (dd, H, J = 7.5 Hz, J = 1.3 Hz), 7.32 (dd, H, J = 8.2 Hz, J = 1.3 Hz), 7.39 (dd, H, J = 8.2 Hz, J = 7.5 Hz), 7.43 (d, H, J = 8.5 Hz), 8.17 (d, H, J = 8.5 Hz) ppm. ^{13}C NMR (100 MHz, [D_4] MeOD): δ = 26.6, 27.1, 27.7 (2C), 28.8 (9C), 29.5 and 30.2 (rotamer), 38.9, 45.7, 48.1 (3C), 50.1, 55.3, 79.9, 80.8, 80.9, 112.1, 118.7, 122.1, 128.2, 129.3, 137.8, 139.3, 154.2, 157.3 (2C), 158.3 (2C). HRMS (MALDI): calcd. for $C_{36}H_{59}N_5O_7$ $[M+H]^+$ 674.4487; found 674.4475.

*Compound (**38**).* Viscous yellow oil (290 mg, 96%). IR (KBr): ν = 3364, 3052, 2974, 2930, 1683, 1600, 1574, 1505, 1471, 1418, 1390, 1366, 1248, 1161, 1086, 871, 835 cm^{-1}. ^1H NMR (400 MHz, [D_4]MeOD): δ = 1.34−1.56 (m, 31H, 2CH_2 9CH_3), 1.68 (qt, 2H, CH_2, J = 6.8 Hz), 1.83 (qt, 2H, CH_2, J = 7.1 Hz), 2.70 (t, 2H, CH_2, J = 6.8 Hz), 3.03 (t, 2H, CH_2, J = 6.8 Hz), 3.14−3.25 (m, 6H, 3CH_2), 3.31 (m, 2H, CH_2), 4.08 (s, 2H, CH_2), 7.09 (dd, H, J = 7.5 Hz, J = 1.3 Hz), 7.34 (dd, H, J = 8.3 Hz, J = 1.3 Hz), 7.40 (dd, H, J = 8.3 Hz, J = 7.5 Hz), 7.45 (d, H, J = 8.5 Hz), 8.19 (d, H, J = 8.5 Hz) ppm. ^{13}C NMR (100 MHz, [D_4]MeOD): δ = 27.1 (2C), 28.6 (3C), 28.7 (3C), 28.8 (3C), 29.7 (2C), 38.9 and 45.4 (rotamer), 45.8, 47.1, 47.9 (2C), 49.8, 55.1, 79.9, 80.9, 81.0, 112.1, 118.8, 122.1, 128.3, 129.4, 137.9, 139.2, 154.2, 157.4 (2C), 158.1, 158.4. HRMS (MALDI): calcd. for $C_{35}H_{57}N_5O_7$ $[M+Na]^+$ 682.4150; found 682.4164.

*Compound (**39**).* Viscous yellow oil (240 mg, 89%). IR (KBr): ν = 3363, 3051, 2973, 2929, 1682, 1600, 1573, 1505, 1471, 1418, 1365, 1250, 1163, 1091, 982, 866, 835 cm^{-1}. ^1H NMR (400 MHz, [D_4]MeOD): δ = 1.42 (bs, 18H, 6CH_3), 1.44 (s, 9H, 3CH_3), 1.68 (qt, 2H, CH_2, J = 6.95 Hz), 1.75 (qt, 2H, CH_2, J = 7.1 Hz), 1.83 (qt, 2H, CH_2, J = 7.1 Hz), 2.69 (t, 2H, CH_2, J = 7.1 Hz), 3.03 (t, 2H, CH_2, J = 6.8 Hz), 3.13−3.25 (m, 6H, 3CH_2), 3.31 (m, 2H, CH_2), 4.07 (s, 2H, CH_2), 7.09 (dd, H, J = 7.5 Hz, J = 1.3 Hz), 7.33 (dd, H, J = 8.3 Hz, J = 1.3 Hz), 7.40 (dd, H, J = 8.3 Hz, J = 7.5 Hz), 7.44 (d, H, J = 8.5 Hz), 8.18 (d, H, J = 8.5 Hz) ppm. ^{13}C NMR (100 MHz, [D_4]MeOD): δ = 28.7 (6C), 28.8 (3C), 29.5 (3C), 38.9, 45.9 (3C), 47.1, 49.8, 55.1, 79.4, 79.9, 81.1, 112.0, 118.8, 122.1, 128.3, 129.3, 137.8, 139.2, 154.2, 157.3 (2C), 158.1, 158.40. HRMS (MALDI): calcd. for $C_{34}H_{55}N_5O_7$ $[M+H]^+$ 646.4174; found 646.4158.

General Procedure for Boc Removal (HQ1-XYZ). To a stirred solution of polyamines **31**−**39** (1 equiv, 0.5 mmol) dissolved in ethanol (3 mL) at 0 °C was added 6 M HCl (3 mL). After 18 h at room temperature, the solution was concentrated in vacuo, and the resulting solid was washed with cold ethanol, filtered, and dried in vacuo to afford Quilamine **40**−**48** as yellow solid, its hydrochloride salt.

*Compound HQ1-**44***. Yellow solid (73%). Mp sup 250 °C. IR (KBr): ν = 3384, 2957, 2798, 1642, 1606, 1551, 1513, 1461, 1420, 1398, 1344, 1302, 1252−1055, 841 cm^{-1}. UV−vis: λ_{max} (nm) ((ε M^{-1} cm^{-1} for pH 7.4), 272 (36300), 307 (2400). ^1H NMR (400 MHz, D_2O): δ = 1.76−2.04 (m, 8H, $4CH_2$), 3.06−3.22 (m, 6H, $3CH_2$), 3.38 (dd, 2H, J = 7.75 Hz, J = 7.45 Hz, CH_2), 4.78 (s, 2H, CH_2), 7.36 (dd, 1H, J = 7.45 Hz, J = 1.49 Hz, H_{7ar}), 7.60 (dd, 1H, J = 8.30 Hz, J = 1.49 Hz, H_{5ar}), 7.65 (dd, 1H, J = 8.30 Hz, J = 7.45 Hz, H_{6ar}), 7.76 (d, 1H, J = 8.60 Hz, H_{3ar}), 8.64 (d, 1H, J = 8.60 Hz, H_{4ar}) ppm. ^{13}C NMR (100 MHz, D_2O): δ = 22.7, 22.8 (2C), 24.0, 38.9, 46.9, 47.0, 47.3, 49.7, 114.1, 119.4, 121.1, 128.9, 129.3, 134.5, 141.8, 148.5, 149.5 ppm. HRMS (MALDI): calcd. for $C_{18}H_{29}N_4O$ [M+H-4HCl]$^+$ 317.2336; found 317.2348. Anal. Calcd for $C_{18}H_{32}Cl_4N_4O{\cdot}1.2\ H_2O$: C, 44.68; H, 7.17; N, 11.58. Found: C, 44.52; H, 6.97; N, 11.57.

*Compound HQ1-**34***. Yellow solid (80%). Mp sup 250 °C. IR (KBr): ν = 3493, 2957, 2770, 2528, 2403, 1599, 1515, 1480, 1458, 1420, 1398, 1304, 859 cm^{-1}. UV−vis: λ_{max} (nm) ((ε M^{-1} cm^{-1} for pH 7.4) 272 (32500), 307 (2100). ^1H NMR (400 MHz, D_2O): δ = 1.66−1.84 (m, 4H, $2CH_2$), 2.17−2.31 (m, 2H, CH_2), 2.97−3.06 (m, 2H, CH_2), 3.07−3.14 (m, 2H, CH_2), 3.15−3.24 (m, 2H, CH_2), 3.41 (m, 2H, CH_2), 4.68 (s, 2H, CH_2), 7.27 (dd, 1H, J = 6.61 Hz, J = 2.43 Hz, H_{7ar}), 7.49−7.57 (m, 2H, H_{5ar} and H_{6ar}), 7.61 (d, 1H, J = 8.50 Hz, H_{3ar}), 8.46 (d, 1H, J = 8.50 Hz, H_{4ar}) ppm. ^{13}C NMR (100 MHz, D_2O): δ = 22.7, 22.8, 23.9, 38.8, 44.5, 44.7, 47.1, 50.5, 113.2, 119.4, 120.8, 128.6, 128.7, 136.1, 139.9, 149.2, 105.4 ppm. HRMS (MALDI): calcd. for $C_{17}H_{27}N_4O$ [M+H-4HCl]$^+$ 303.2179; found 303.2183. Anal. Calcd for $C_{17}H_{30}C_{l4}N_4O{\cdot}0.4H_2O$: C, 41.89; H, 6.37; N, 11.47. Found: C, 42.15; H, 6.36; N, 11.16.

*Compound HQ1-**43***. Yellow solid (88%). Mp sup 250 °C. IR (KBr): ν = 3039, 2984, 2825, 1641, 1606, 1538, 1461, 1419, 1402, 1352, 1302, 842 cm^{-1}. UV−vis: λ_{max} (nm) ((ε M^{-1} cm^{-1} for pH 7.4) 272 (34500), 307 (2200). ^1H NMR (400 MHz, D_2O): δ = 1.84−2.05 (m, 4H, $2CH_2$), 2.11−2.22 (m, 2H, CH_2), 3.14−3.27 (m, 6H, $3CH_2$), 3.34−3.41 (m, 2H, CH_2), 4.75 (s, 2H, CH_2), 7.39 (dd, 1H, J = 6.5 Hz, J = 2.4 Hz, H_{7ar}), 7.62−7.70 (m, 2H, H_{5ar} and H_{6ar}), 7.71 (d, 1H, J = 8.5 Hz, H_{3ar}), 8.59 (d, 1H, J = 8.5 Hz, H_{4ar}) ppm. ^{13}C NMR (100 MHz, D_2O): δ = 22.8, 22.9, 23.8, 36.6, 44.6, 47.0, 47.1, 50.3, 113.3, 119.4, 120.9, 128.8 (2C), 135.8, 140.2, 149.3, 150.3 ppm. HRMS (MALDI): calcd. for $C_{17}H_{27}N_4O$ [M+H-4HCl]$^+$ 303.2179; found 303.2190. Anal. Calcd for $C_{17}H_{30}Cl_4N_4O{\cdot}1.1\ H_2O$: C, 43.62; H, 6.93; N, 11.97. Found: C, 43.4; H, 6.71; N, 12.19.

*Compound HQ1-**33***. Yellow solid (76%). Mp sup 250 °C. IR (KBr): ν = 3423, 2962, 2760, 2692, 1636, 1607, 1595, 1517, 1458, 1397, 1303, 1272, 1094, 842 cm^{-1}. UV−vis: λ_{max} (nm) ((ε $M^{-1}cm^{-1}$ for pH 7.4) 272 (36200), 307 (2200). ^1H NMR (400 MHz, D_2O): δ = 2.12−2.22 (m, 2H, CH_2), 2.28−2.39 (m, 2H, CH_2), 3.14−3.21 (m, 2H, CH_2), 3.22−3.34 (m, 4H, $2CH_2$), 3.42−3.49 (m, 2H, CH_2), 4.80 (s, 2H, CH_2), 7.37 (dd, 1H, J = 7.28 Hz, J = 1.46 Hz, H_{7ar}), 7.61 (dd, 1H, J = 8.37 Hz, J = 1.64 Hz, H_{5ar}), 7.66 (dd, 1H, J = 7.46 Hz, J = 7.28 Hz, H_{6ar}), 7.75 (d, 1H, J = 8.55 Hz, H_{3ar}), 8.63 (d, 1H, J = 8.55 Hz, H_{4ar}) ppm. ^{13}C NMR (100 MHz, D_2O): δ = 22.7, 23.7, 36.6, 44.7, 44.8, 44.9, 49.9, 114.0, 119.4, 121.1, 128.9, 129.2, 134.7, 141.6, 148.5, 149.7 ppm. HRMS (MALDI): calcd. for $C_{16}H_{25}N_4O$ [M+H-4HCl]$^+$ 289.2023; found 289.2034. Anal. Calcd for $C_{16}H_{28}Cl_4N_4O{\cdot}1.45\ H_2O$: C, 41.74; H, 6.77; N, 12.17. Found: C, 41.59; H, 6.58; N, 12.17.

*Compound HQ1-**444***. Yellow solid (95%). Mp sup 250 °C. IR (KBr): ν = 3426, 3038, 2956, 2874, 2799, 2758, 1642, 1606, 1598, 1449, 1302 cm^{-1}. UV−vis: λ_{max} (nm) ((ε M^{-1} cm^{-1} for pH 7.4) 272 (34500), 307 (2000). ^1H NMR (400 MHz, D_2O): δ = 1.75−2.03 (m, 12H, $6CH_2$), 3.06−3.22 (m, 10H, $5CH_2$), 3.34−3.41 (m, 2H, CH_2), 4.78 (s, 2H, CH_2), 7.39 (dd, 1H, J = 7.15 Hz, J = 1.79 Hz, H_{7ar}), 7.61−7.71 (m, 2H, H_{5ar} and H_{6ar}), 7.77 (d, 1H, J = 8.54 Hz, H_{3ar}), 8.65 (d, 1H, J = 8.54 Hz, H_{4ar}) ppm. ^{13}C NMR (100 MHz, D_2O): δ = 22.7, 22.8 (4C), 24.0, 38.9, 46.9 (3C), 47.0, 47.3, 49.8, 114.0, 119.4, 121.1, 128.9, 129.2, 134.8, 141.5, 148.7, 149.7 ppm. HRMS (MALDI): calcd. for $C_{22}H_{38}N_5O$ [M+H-5HCl]$^+$ 388.3071; found 388.3059. Anal. Calcd for $C_{22}H_{42}Cl_5N_5O$ 1.7 H_2O: C, 44; H, 7.62; N, 11.66. Found: C, 43.64; H, 7.45; N, 12.05.

*Compound HQ1-**443***. Yellow solid (91%). Mp sup 250 °C. IR (KBr): ν = 3441, 2951, 2777, 2577, 2421, 1641, 1597, 1515, 1477, 1451, 1418, 1401, 1352, 1301, 1247, 1232, 1209, 1168, 1092, 1056, 841 cm^{-1}. UV−vis: λ_{max} (nm) ((ε M^{-1} cm^{-1} for pH 7.4) 272 (35300), 307 (2000). ^1H NMR (400 MHz, D_2O): δ = 1.81−2.02 (m, 8H, $4CH_2$), 2.12−2.21 (m, 2H, CH_2), 3.12−3.27 (m, 10H, $5CH_2$), 3.35−3.39 (m, 2H, CH_2), 4.77 (s, 2H, CH_2), 7.39 (dd, 1H, J = 6.9 Hz, J = 2 Hz, H_{7ar}), 7.63−7.71 (m, 2H, H_{5ar} and H_{6ar}), 7.75 (d, 1H, J = 8.6 Hz, H_{3ar}), 8.63 (d, 1H, J = 8.6 Hz, H_{4ar}) ppm. ^{13}C NMR (100 MHz, D_2O): δ = 22.8 (2C), 22.9 (2C), 23.8, 36.6, 44.6, 46.9 (2C), 47.1, 47.2, 50.1, 113.7, 119.4, 121.1, 128.9, 129.1, 135.2, 141.0, 148.9, 149.9 ppm. HRMS (MALDI): calcd. for $C_{21}H_{36}N_5O$ [M+H-5HCl]$^+$ 374.2914; found 374.2927. Anal. Calcd for $C_{21}H_{40}Cl_5N_5O{\cdot}1.35\ H_2O$: C, 43.48; H, 7.42; N, 12.07. Found: C, 43.32; H, 7.25; N, 12.22.

*Compound HQ1-**344***. Yellow solid (92%). Mp sup 250 °C. IR (KBr): ν = 3416, 2954, 2770, 2441, 1631, 1602, 1512, 1456, 1412, 1351, 1312, 1249, 1168, 1095, 1056 cm^{-1}. UV−vis: λ_{max} (nm) ((ε M^{-1} cm^{-1} for pH 7.4) 272 (36900), 307 (2200). ^1H NMR (400 MHz, D_2O): δ = 1.77−1.92 (m, 8H, $4CH_2$), 2.28−2.39 (m, 2H, CH_2), 3.07−3.23 (m, 8H, $4CH_2$), 3.25−3.32 (m, 2H, CH_2), 3.41−3.47 (m, 2H, CH_2), 4.74 (s, 2H, CH_2), 7.35 (dd, 1H, J = 6.6 Hz, J = 2.3 Hz H_{3ar}), 7.60−7.66 (m, 3H,), 8.49 (d, 1H, J = 8.6 Hz) ppm. ^{13}C NMR (100 MHz, D_2O): δ = 22.7, 22.8 (3C), 23.9, 38.8, 44.5, 44.6, 46.8, 46.9, 47.1, 50.8, 112.7, 119.4, 120.6, 128.4, 128.6, 136.6, 139.1, 149.5, 150.7 ppm. HRMS (MALDI): calcd. for $C_{21}H_{36}N_5O$ [M+H-5HCl]$^+$ 374.2914; found 374.2905. Anal. Calcd for $C_{21}H_{40}Cl_5N_5O{\cdot}0.3\ H_2O$: C, 44.94; H, 7.29; N, 12.48. Found: C, 44.7; H, 7.15; N, 12.72.

*Compound HQ1-**343***. Yellow solid (92%). Mp sup 250 °C. IR (KBr): ν = 3386, 2957, 2776, 2425, 1642, 1606, 1312, 1461, 1413, 1348, 1303, 1252, 1111, 1093, 1058 cm^{-1}. UV−vis: λ_{max} (nm) ((ε M^{-1} cm^{-1} for pH 7.4) 272 (34500), 307 (2100). ^1H NMR (400 MHz, D_2O): δ = 1.81−1.91 (m, 4H, $2CH_2$), 2.12−2.22 (m, 2H, CH_2), 2.28−2.38 (m, 2H, CH_2), 3.13−3.32 (m, 10H, $5CH_2$), 3.41−3.48 (m, 2H, CH_2), 4.79 (s, 2H, CH_2), 7.38 (dd, 1H, J = 7 Hz, J = 1.93 Hz), 7.61−7.69 (m, 2H, CH_2), 7.74 (d, 1H, J = 8.6 Hz, H_{3ar}), 8.61 (d, 1H, J = 8.6 Hz, H_{4ar}) ppm. ^{13}C NMR (100 MHz, D_2O): δ = 22.7, 22.8 (2C), 23.8, 36.6, 44.5, 44.6 (2C), 44.8, 47.1, 50.2, 113.7, 119.4, 121.0, 128.9, 129.1, 135.3, 140.5, 148.8, 150.0 ppm. HRMS (MALDI): calcd. for $C_{20}H_{34}N_5O$ [M+H-5HCl]$^+$ 360.2758; found 360.2764. Anal. Calcd for $C_{20}H_{38}Cl_5N_5O{\cdot}0.7\ H_2O$: C, 43.33; H, 7.16; N, 12.63. Found: C, 43.05; H, 7.14; N, 12.97.

*Compound HQ1-**333***. Yellow solid (96%). Mp sup 250 °C. IR (KBr): ν = 3424, 2963, 2756, 2696, 2585, 2420, 1636, 1607, 1594, 1550, 1519, 1458, 1402, 1303, 1265, 1094 cm^{-1}. UV−vis:

λ_{max} (nm) ((ε M^{-1} cm^{-1} for pH 7.4) 272 (35400), 307 (2100). ^{1}H NMR (400 MHz, D_2O): δ = 2.12−2.26 (m, 4H, $2CH_2$), 2.29−2.39 (m, 2H, CH_2), 3.14−3.36 (m, 10H, $2CH_2NHCH_2$ and CH_2NH_2), 3.42−3.49 (m, 2H, NH CH_2), 4.79 (s, 2H, CH_2), 7.38 (dd, 1H, J = 6.8 Hz, J = 2 Hz, H_{7ar}), 7.61−7.69 (m, 2H, CH_2, H_{5ar} and H_{6ar}), 7.73 (d, 1H, J = 8.6 Hz, H_{3ar}), 8.61 (d, 1H, J = 8.6 Hz, H_{4ar}) ppm. ^{13}C NMR (100 MHz, D_2O): δ = 22.6, 22.7, 23.8, 36.6, 44.6, 44.7, 44.8 (3C), 50.3, 113.5, 119.4, 120.9, 128.8, 128.9, 135.5, 140.6, 148.6, 150.1 ppm. HRMS (MALDI): calcd. for $C_{19}H_{32}N_5O$ $[M+H-5HCl]^+$ 346.2601; found 346.2614. Anal. Calcd for $C_{19}H_{36}Cl_5N_5O{\cdot}0.85\ H_2O$: C, 42.02; H, 7; N, 12.9. Found: C, 42.13; H, 6.82; N, 12.73.

Study of the Acid−Base and Metal Complexation Properties of Quilamine HQ1-44. Potentiometric titrations were performed in a glass-jacketed titration cell thermostated at 25 ± 0.1 °C and closed under an inert gas atmosphere, using a Metrohm 702 SM Titrino titration stand connected to a Metrohm 6.0233.100 combined glass electrode and controlled by the *Metrohm Tinet 2.4* software. The titrant was a carbonate-free KOH solution at approximately 0.1 M prepared from a commercial ampule of analytical grade, and its exact concentration was obtained by titration of a standard HNO_3 solution. A stock solution of **HQ1−44** was prepared at ∼1.5 × 10^{-3} M. Stock solutions of iron(III), copper(II), zinc(II), and magnesium(II) cations were prepared at ∼0.05 M from the analytical grade salts $FeCl_3$, $CuCl_2$, $Zn(NO_3)_2$, and $MgSO_4$, and were standardized by complexometry against a standard EDTA (ethylenediaminetetraacetic acid) solution. Sample solutions contained ∼0.03 mmol of ligand in a total volume of 30 mL, with the ionic strength kept at 0.10 M using KNO_3 as background electrolyte. Complexation titrations were run by addition of approximately 0.5 or 1 equiv for iron(III) and copper(II), or 1 equiv for zinc(II) and magnesium(II). The $[H^+]$ of the solutions was determined by measurement of the electromotive force of the cell, $E = E^{\circ\prime} + Q \log[H^+] + E_j$. The term pH is defined as $-\log [H^+]$, and a value of K_w = $[H^+][OH^-]$ = $10^{-13.778}$ was taken from the literature for our experimental conditions. $E^{\circ\prime}$ and Q were determined by titrating a standard HNO_3 solution at the same ionic strength. The liquid-junction potential, E_j, was found to be negligible under the experimental conditions used. Each titration consisted of 150−200 equilibrium points in the range of pH 2.0−11.5, and at least two replicate titrations were performed for each individual system. The potentiometric data were refined with the *Hyperquad* software, and speciation diagrams were plotted using the *Hyss* software. The overall equilibrium (formation) constants β_i^H and β_{MmHhLl} are defined by $\beta_{MmHhLl=[MmHhLl]/[M]m[H]h[L]l}$ and $\beta_{MH-1\ L=}$ $\beta_{ML(OH)}$ × K_w, while stepwise equilibrium constants are given by $K_{MmHhLl=[MmHhLl]/[MmHh-1Ll][H]}$ and correspond to the difference in log units between overall constants of sequentially protonated (or hydroxide) species. The pM values for each metal complex were calculated from the full set of stability constants of each system at pH = 7.4 with c_L = 1.0 × 10^{-5} M and c_M = 1.0 × 10^{-6} M.

BIOLOGY

Chelator Solutions. All reagents, which were of the highest available grade, were obtained from Sigma-Aldrich Chimie (Saint Quentin Fallavier, France). All synthesized Quilamines were compared to the tridentate iron-chelator hydroxyphenyl-triazole ICL670 as a reference (Deferasirox, Exjade from Novartis Pharma) as well as to the 8-hydroxyquinoline. Stock solutions of each chelator (10 mM) were prepared in water. The high solubility of each derivative in culture medium in the concentration range 0−400 μM was preliminary verified by turbidimetry measurement. Three controls have been done for each experiment: one with the standard culture medium, and the other with culture medium. When chelator treatment was performed in the presence of exogenous iron, they have been iron saturated with 20 μM ferric iron ($FeCl_3$). Unbound iron was not removed from the medium. NTBI is classically used to induce iron overload in various cells because it represents the plasma iron species which is mainly responsible for creating parenchymal (especially hepatocyte) iron deposition in human chronic iron overload.

Comparison of Chelator Efficiency in Aqueous Phase, Competition with Calcein. Fluorescence emission (λ_{Exc} = 485 nm, λ_{Em} = 520 nm) of calcein (100 nM) in an HEPES buffer (20 mM HEPES, 150 mM NaCl, pH 7.3) was measured at room temperature in a microplate fluorescence reader (Packard, Fusion), equipped with an orbital stirring. Iron(III) (1 μM) slowly reacted with calcein and maximal quenching of its fluorescence was observed for time longer than 6 h. The fluorescence recovery was monitored after 4 h incubation in the presence of various chelator concentrations. In the absence of iron, various chelators slightly modulated the calcein fluorescence intensity. Results were expressed as a percentage of fluorescence recovery with respect to the free calcein fluorescence intensity measured in the absence of iron.

Cells Studies. The involvement of the PTS in the selective uptake of Quilamines was investigated by using Chinese hamster ovary cells (CHO) exhibiting high PTS activity[46] and the mutated derived-cell line CHO-MG cells, devoided of PTS (provided by Dr. W. Flintoff, University of Western Ontario). The CHO-MG cell was selected for growth resistance to methylglyoxalbis-(guanylhydrazone), using a single-step selection after mutagenesis with ethyl methanesulfonate. Therefore, highly selective PTS ligands should give high (CHO-MG/CHO) IC_{50} ratios.

The two cell lines were grown in RPMI 1640 medium, supplemented with 10% fetal calf serum (Eurobio, Les Ulis, France), 2 mM Glutamine (Bio Media, Boussens, France), 100 units/mL penicillin, and 50 μg/mL streptomycin, at 37 °C in 5% humidified CO_2. L-Proline (2 μg/mL) was added to the culture medium for CHO-MG cells.

Cell Treatment. For experiments, cells were harvested with trypsin and seeded 24 h before the polyamine treatment in 96-well microplates (Becton Dickinson, Oxnard, CA) at a density of 2000 cells per well. In these conditions, cells reached confluency in 5−6 days. Chelator exposure was performed one day after cell seeding in proliferating CHO and CHO-MG cells. The effect of Quilamines on cell viability was also tested in the presence of DFMO (1 mM), a selective inhibitor of ODC which induced a depletion of intracellular putrescine and spermidine and leads to an activation of the PTS. In this assay, the cells were seeded in the presence of the inhibitor. In other experiments, 50 μM spermidine was added to the culture medium to inhibit by a competitive inhibition, the active uptake of Quilamines from PTS. To prevent the oxidation of the exogenous polyamine by the serum amine oxidase present in the fetal calf serum, aminoguanidine (1 mM), an inhibitor of this enzyme, was added to the medium. The various derivatives were compared to the tridentate iron chelator hydroxyphenyl-triazole ICL670 (Deferasirox, Exjade) and to the bidentate 8-hydroxyquinoline.

Cytostatic and Cytotoxic Effects Measurements. Chelator exposure was performed one day after cell seeding in proliferating CHO and CHO-MG cells. After 72 h incubation at 37 °C, cell supernatants were collected for cytotoxicity measurement by measuring extracellular LDH activity (cytotoxicity detection kit − LDH, Roche, Penzberg, Germany). Extracellular LDH activity was measured as described by the manufacturer on a 20 μL aliquot of cell free medium obtained by centrifugation (2500 rpm/min during 5 min). LDH activities were detected by reading absorbance at 485 nm. They were reported as a percentage of extracellular LDH activity with respect to the control value.

Cell viability was determined by counting the cell nuclei after staining with the fluorescent DNA intercalating dye Hoechst 33342. The treated CHO and CHO-MG cells were washed twice with PBS (50 mM pH 7) and fixed with ethanol/acetic acid during 20 min at 4 °C. Cells were counterstained 10 min with Hoechst 33342 dye diluted by 1/1000 (5 μg/mL) in PBS and images were taken with an upright microscope (AxioImager M1, Zeiss, France). Images analysis and cell nuclei counting was performed with the simple *PCI* software (C Imaging Image Analysis System, Compix, USA). The number of cell nuclei was reported as a percentage of the control value. Parameters of the dose−response curves were deduced from a four-parameter curve fit according to Rodbard[47]

$$y = \frac{(A_{cmin} - A_{cmax})}{1 + \left(\frac{C}{C_{ip}}\right)P_{ip}} + A_{cmax}$$

in which y is the percentage of cell nuclei number with respect to the control, A_{Cmin} and A_{Cmax} are the y values observed for minimal and maximal chelator concentrations respectively, C is the chelator concentration (C_{ip} at the inflection point), and P_{ip} is the slope at inflection point of the sigmoid curve. Due to their biphasic feature, the dose−response curves were fitted as the sum of two sigmoids (double 4-parameter fit). Percentages of CHO and CHO-MG cells involved in each viability responses were deduced from the A_{Cmin}, A_{Cmax}, and IC_{50} values of each sigmoid, which were obtained from these fits.

Three independent replicates were performed for each experiment, which was repeated three times.

Computational Details. As its computational cost is in the same order of the Hartree−Fock (HF) method, DFT is applicable to much larger systems than the correlated *ab initio* methods. DFT theory has been used to obtain the structure and energy of all the compounds under study. We have selected for our calculations OPBE, one of the best performing exchange-correlation functional for the iron complexes,[48] which is the combination of Handy's optimized exchange (OPTX)[49] with the PBE correlation.[50] The 6-31G(d,p) basis set, a double-ζ Pople-type basis set for H,C N,O, and Cl atoms and the Lanl2DZ (Los Alamos National Laboratory 2 double-ζ) with effective core potentials (ECP) for Fe atom are employed in the present investigation.

The DFT calculations were carried out with the *Gaussian 09* software package.[51] All open-shell structures were calculated with unrestricted DFT method, whereas for closed-shell molecules, the restricted DFT method was employed. Calculations of iron complexes were performed for spin multiplicities 2, 4, and 6. The Fe(III) complexes were optimized, often using distinct geometries by placing the ligands in pseudo-octahedral orientation about the metal as starting points. These starting points have led to the most stable geometries presented below. The existence of local minima was checked by inspection of the Hessian matrix eigenvalues. For all iron complexes, the stability of the wave function was checked. Unscaled values were used for zero-point vibrational energy corrections for energy values. Thermal corrections were calculated for the evaluation of reaction enthalpies ΔH and Gibbs energies ΔG at 298.15 K, using standard statistical mechanic formulas in the independent mode, harmonic oscillator, and rigid rotor approximations.

RESULTS AND DISCUSSION

Chemistry. We first developed a synthetic protocol to tether 8-hydroxyquinoline-2-carbaldehyde to a set of linear polyamines by reductive amination (Figure 1).

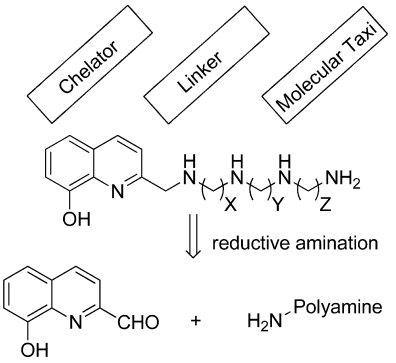

Figure 1. Quilamine **HQ1-*XYZ*** synthesis.

To optimize the efficiency of this novel family of Quilamines in terms of cytotoxicity and PTS selectivity, we studied the influence of the number of nitrogen atoms present in the polyamine chain and the distance between them. The synthesis of nine protected spermidine and spermine analogues described in Figure 2 was carried out. Diverse methodologies for the

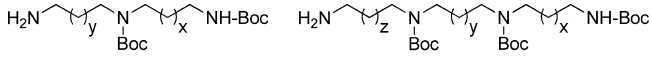

x=2, y=2 : homospermidine **1**
x=2, y=1 : spermidine **2**
x=1, y=2 : spermidine **3**
x=1, y=1 : norspermidine **4**

x=2, y=2, z=2 : dihomospermine **5**
x=1, y=2, z=2 : homospermine **6**
x=2, y=2, z=1 : homospermine **7**
x=1, y=2, z=1 : spermine **8**
x=1, y=1, z=1 : norspermine **9**

Figure 2. Structure of protected spermidine and spermine analogues **1**−**9**.

synthesis of polyamine have recently been reported in the literature.[52−54] We selected an iterative approach involving cyano-alkylation followed by nitrile reduction.[45,55,56]

The spermidine analogues **1**−**4** were prepared according to a modified four-step procedure providing good yields (Scheme 1).

The first step consisted of reacting putrescine or 1,3-diaminopropane with di-*tert*-butyl dicarbonate (Boc_2O) leading to monoprotected diamines **10** and **11**, respectively. Amine **10** was reacted with 4-bromobutyronitrile to give secondary amine **12**, followed by quantitative Boc-protection giving rise to compound **13**. The nitrile was reduced by hydrogenation with Raney Ni to give masked homospermidine **1** with an overall yield of 63%. This procedure represents an improved yield compared to a previously described protocol (44% yield).[31,57]

Scheme 1. Synthesis of Spermidine Analogues 1−4[a]

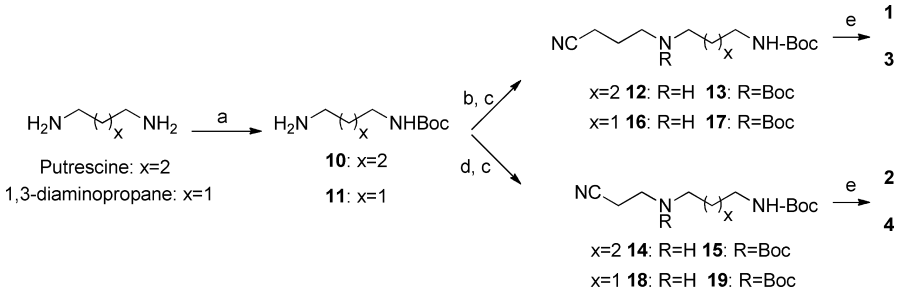

[a]Reagents: (a) $(Boc)_2O$ (0.33 equiv), Et_3N, MeOH, 0 °C to r.t., 20 h; (b) 4-bromobutyronitrile (1 equiv), K_2CO_3, CH_3CN, 50 °C, 12 h; (c) $(Boc)_2O$ (2.5 equiv), Et_3N, MeOH, r.t., 20 h; (d) acrylonitrile (1 equiv), MeOH, 0 °C, 14 h; (e) H_2, Raney Ni, EtOH, NH_4OH, 20 atm, r.t., 12 h.

Scheme 2. Synthesis of Spermine Analogues 5−9[a]

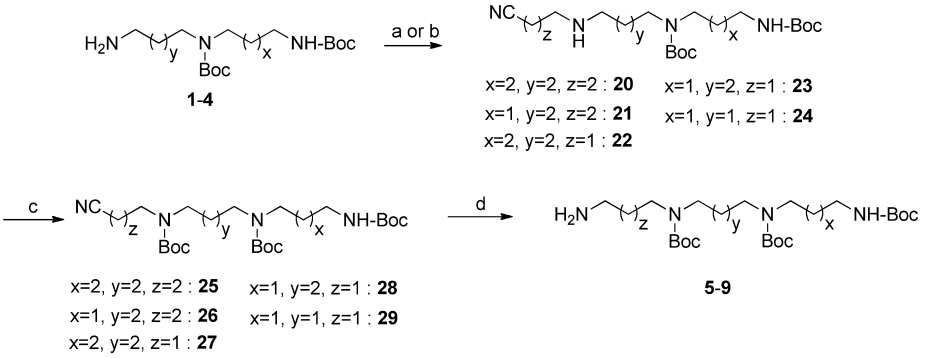

[a]Reagents: (a) 4-bromobutyronitrile (1 equiv), K_2CO_3, CH_3CN, 50 °C, 12 h; (b) acrylonitrile (1 equiv), MeOH, 0 °C, 14 h; (c) $(Boc)_2O$ (2.5 equiv), Et_3N, MeOH, r.t., 20 h; (d) H_2, Raney Ni, EtOH, NH_4OH, 20 atm, r.t., 12 h.

N^4,N^8-Di-*tert*-butyloxycarbonylspermidine **2** was prepared, still from amine **10**, which was alkylated this time via a Michael-addition on acrylonitrile with a yield of 96%. Boc protection of the resultant secondary amine **14** provided nitrile **15**. Treatment with Raney Ni under 20 atm of hydrogen induced the expected nitrile reduction in quantitative yield with no further purification required. This method proved to be more suitable than that described by Paul M. O'Neill in 2010, which used $LiAlH_4$ as reagent and provided yields of no more than 24%.[58] With this protocol, di-Boc-spermidine **2** was obtained with a significantly higher overall yield than previously described (74% vs 32%).[59] N^1,N^4-Di-*tert*-butyloxycarbonylspermidine **3** and norspermidine **4** were prepared in the same manner from Boc-protected diamine **11** with an overall yield of 49% and 78%, respectively.

Dihomospermine **5**, homospermines **6** and **7**, spermine **8**, and norspermine **9** were designed as homologues of **1**−**4**, where the N^1-tether was sequentially lengthened. Compounds **5**−**9** were prepared similarly to the di-Boc spermidine analogues in three steps (Scheme 2). Spermine skeletons **1**−**4** were first alkylated with bromobutyronitrile or acrylonitrile to give compounds **20**−**24**. After protection of the secondary amino group with di-*tert*-butyl dicarbonate, compounds **25**−**29** were converted into the expected spermines **5**−**9** with excellent yields (84−95%).

With protected polyamines **1**−**9** in hand, we decided to evaluate a reductive-amination protocol with 8-hydroxyquinoline-2-carbaldehyde to form the Quilamines **HQ1**-*XYZ*. 8-Hydroxyquinoline-2-carbaldehyde **30** was obtained in three steps according to methods previously described in the literature (Scheme 3).[60]

8-Hydroxyquinaldine was protected as the silylether by treatment with *tert*-butyldimethylsilyl chloride in the presence of imidazole, followed by an oxidation of the methyl group by selenium dioxide in 1,4-dioxane to yield the corresponding aldehyde in 90% yield. After deprotection of phenol by treatment with an excess of *tetra-n*-butylammonium fluoride in THF, the 8-hydroxyquinoline-2-carbaldehyde **30** was isolated with an overall yield of 66%. The reductive amination of this aldehyde with a range of polyamines **1**−**9** was achieved in one pot by using sodium triacetoxyborohydride for reduction of the imine generated *in situ*.[61] Protected intermediates **31**−**39** were isolated in good yields (82−96%). Removal of the Boc-protecting groups under acidic conditions at room temperature gave the polyaminoquinoline **HQ1**-*XYZ* as hydrochloride salts. These nine new Quilamines were fully characterized by a combination of the usual techniques (IR, UV−vis, MS, elemental analysis, ^{13}C and ^{1}H NMR) and fulfilled the purity required for the biological evaluations.

Biological Evaluations. *Cytostatic (Antiproliferative) and Cytotoxic Effects of Chelators.* Quilamines **HQ1**-*XYZ* were screened for their antiproliferative activity and cytotoxicity in CHO (Chinese Hamster Ovary) cells which exhibit high PTS activity[62] and the mutated derived-cell line CHO-MG cells, devoid of the PTS (provided by Dr. W. Flintoff, University of Western Ontario). CHO cells and the CHO-MG cell line were chosen to evaluate the potential role of the PTS as a selective transport system. We assessed the antiproliferative activity of the various compounds by measuring DNA content after Hoescht staining. The release of the cytoplasmic protein lactate dehydrogenase (LDH) into cell supernatants was used as a marker of cell membrane disruption correlated to cytotoxicity.

dx.doi.org/10.1021/bc300324c | *Bioconjugate Chem.* 2012, 23, 1952−1968

Scheme 3. Synthesis of Quilamines HQ1-*XYZ*[a]

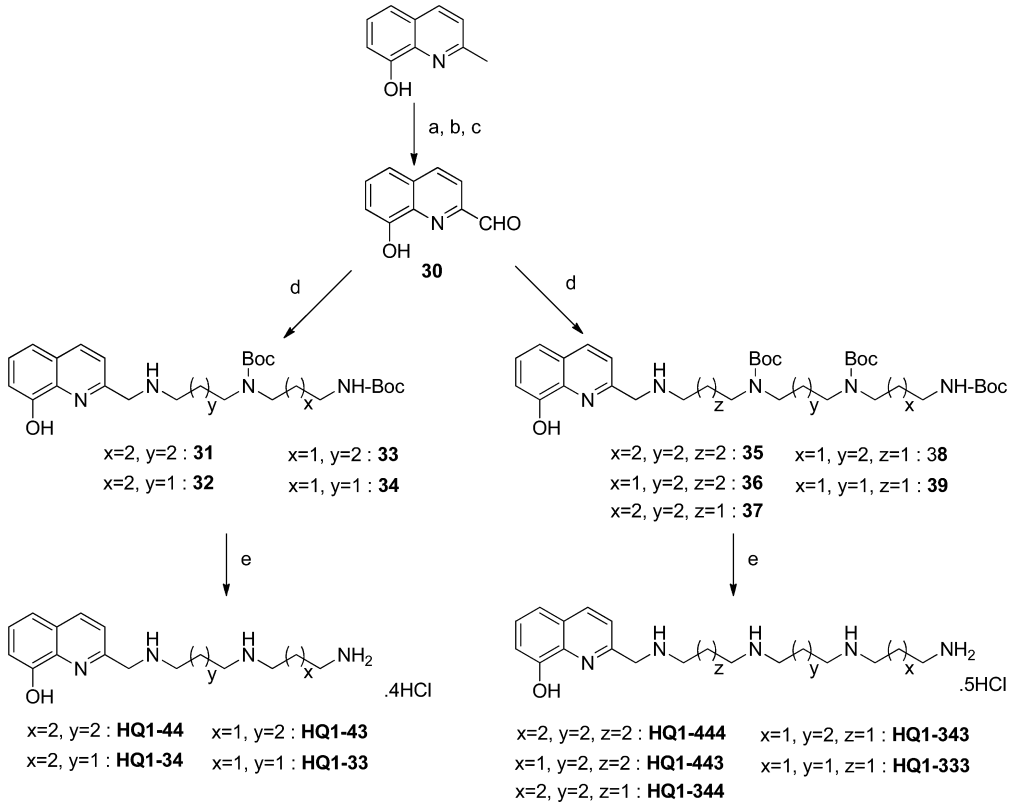

[a]Reagents: (a) TBDMSCl (1.1 equiv), imidazole (1.1 equiv), CH_2Cl_2, r.t., 12 h; (b) selenium dioxide (1.2 equiv), 1,4-dioxane, 90 °C, 90 min; (c) TBAF (1.5 equiv), THF, r.t., 2 h; (d) polyamines **1**–**9**, $NaBH(OAc)_3$ (3 equiv), $C_2H_4Cl_2$, r.t., 12 h; (e) HCl 6 M, EtOH, r.t., 20 h.

The dose–response curves deduced from the counting of cell nuclei by Hoescht fluorescence in proliferating CHO cells were biphasic for the various Quilamines, including **HQ1–44** shown as an example in Figure 3A, except **HQ1–43**, **HQ1–343**, **HQ1–333**, and the reference chelator 8-hydroxyquinoline (8-HQ). They were fitted as a double four-parameter fit to calculate the percentage of cells involved in each viability component, the cytostatic (C1) and cytotoxic ones (C2), as well as their corresponding IC_{50} (Table 1). Dose–effect curves of the extracellular LDH released into the supernatant, expressed in relation to the untreated CHO and CHO-MG control cells, are reported in Figure 3B for **HQ1–44** and the two reference chelators (8-HQ and ICL670). The decrease in cell viability observed with 8-HQ (Figure 3A) was associated with a cytotoxic effect leading to LDH leakage (Figure 3B), while that observed with ICL670 and **HQ1–44** at concentrations lower than 10 μM corresponded to a cytostatic effect (no LDH release). LDH values for compound concentrations in the range of the cytostatic component **1** (10 μM) and the cytotoxic component **2** (100 μM) are also reported in Table 1.

The low concentration component 1 involved 80%, 55%, 35%, 60%, 30%, and 18% of CHO cells treated with **HQ1–44** (IC_{50-1} = 1.2 μM), **HQ1–444** (IC_{50-1} = 1.8 μM), **HQ1–443** (IC_{50-1} = 1.0 μM), **HQ1–33** (IC_{50-1} = 2.0 μM), **HQ1–34** (IC_{50-1} = 20.0 μM), and **HQ1–344** (IC_{50-1} = 2.0 μM), respectively; and only 20% of CHO cells treated by ICL670 (IC_{50-1} = 3.0 μM). As deduced from the absence of LDH leakage into supernatants, the chelator treatments at 10 μM were not cytotoxic and probably reflected the antiproliferative activity of the various compounds. In contrast, the second component of the dose–effect curves was associated with membrane damage and LDH release for a concentration of 100 μM and corresponded to the cytotoxicity of the various Quilamines and the reference chelators (8-HQ and ICL670). In nonproliferative CHO cells, treated with the various compounds at confluency (data not shown), the dose–response curves of cell viability were monophasic, with IC_{50} higher than 50–100 μM, and reflected only their cytotoxicity (LDH release).

The antiproliferative efficiency of the various Quilamines, deduced from the percentage of the low concentration component 1 (IC_{50-1} < 10 μM) was in the following order: **HQ1–44** (80%) > **HQ1–33** (60%) ~ **HQ1–444** (55%) > **HQ1–443** (35%) > **HQ1–34** (30%) > **HQ1–344** (18%) > **HQ1–333** ~ **HQ1–43** ~ **HQ1–343**. The Quilamine **HQ1–44** exhibited the highest antiproliferative activity and the lowest cytotoxicity with respect to all the other compounds, including the reference chelator ICL670 (20%, IC_{50} = 3.0 μM).

*Selectivity for the Polyamine Transport System (**PTS**).* When cell viability was analyzed without multicomponent analysis, the dose–effect curves obtained with Quilamine **HQ1–44** showed overall IC_{50} values of 1.4 μM and 344 μM in the CHO and mutated PTS deficient CHO-MG cell line, respectively (Figure 3A and Table 2). The antiproliferative effect of this compound **HQ1–44** was observed in the micromolar range, while its cytotoxicity, which was detected by membrane damage (LDH release, Figure 3B), was observed only for concentrations higher than 100 μM in both CHO and CHO-MG cell lines.

dx.doi.org/10.1021/bc300324c | *Bioconjugate Chem.* 2012, 23, 1952–1968

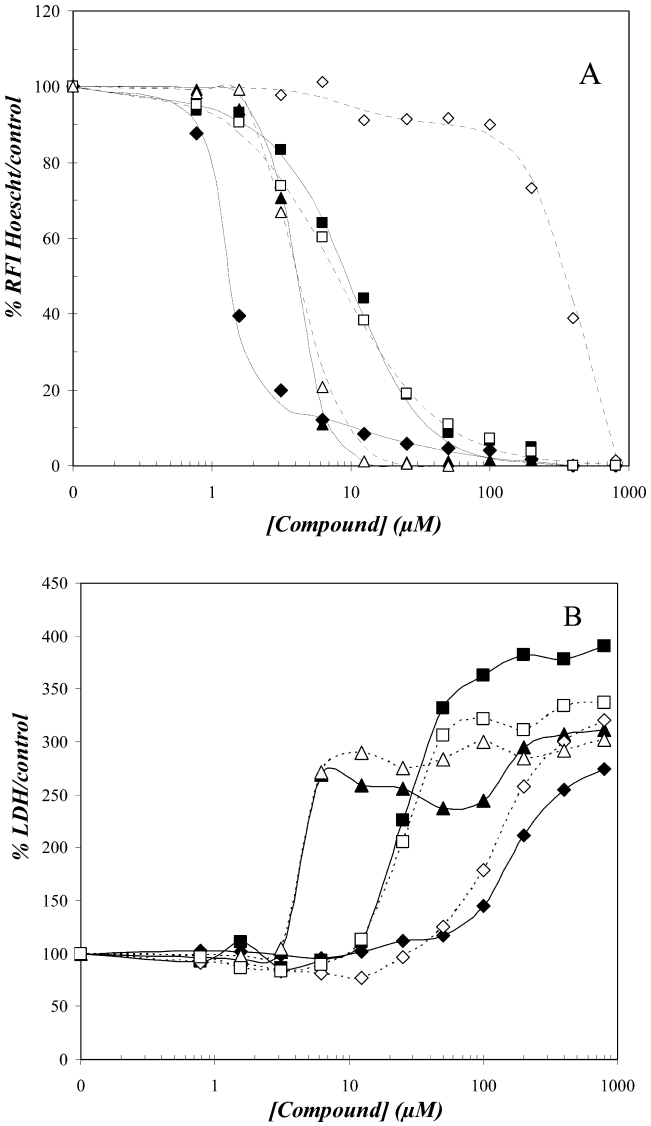

Figure 3. Cytostatic and cytotoxic effects of **HQ1−44**, 8-HQ, and ICL670 in the CHO (solid lines) and CHO-MG cell lines (dotted lines). The cytostatic effect was determined by measuring DNA content after Hoescht staining (A). The cytotoxic effect was evaluated by measuring LDH leakage into the culture medium (B). ◆ **HQ1−44** (CHO), ◇ **HQ1−44** (CHO-MG), ■ ICL670 (CHO), □ ICL670 (CHO-MG), ▲ 8-HQ 5CHO), Δ 8-HQ (CHO-MG) for A and B.

Due to the absence of a polyamine chain, the two reference chelators, 8-HQ and ICL670, were not imported by the PTS and showed an equivalent efficiency in the two cell lines with a CHO-MG/CHO IC_{50} ratio equal to 1. In contrast, a high value of this IC_{50} ratio was characteristic of a high PTS selectivity (Table 2). The Quilamine **HQ1−44**, which presents an exceptionally high CHO-MG/CHO IC_{50} ratio (249), was the one most efficiently imported into the CHO cells due to its strong selectivity of recognition by the PTS. Exogenous spermidine (50 μM), which induced a competitive inhibition of the **HQ1−44** uptake by the PTS, decreased the antiproliferative efficiency of this Quilamine in CHO cells (Figure S1, ESI). Conversely, the activation of the PTS induced by a DFMO pretreatment increased the cytostatic effect of **HQ1−44**. Both DFMO and exogenous spermidine treatments were ineffective at modulating the cytotoxic effect of **HQ1−44** on CHO-MG cells (data not shown). These results strongly suggest that the antiproliferative capacity of the various Quilamines depends mainly on their cell uptake by the PTS. Quilamines bearing a 44 polyamine chain (**HQ1−44**, **HQ1−444**) were more selectively recognized by the PTS than those bearing a 33 chain (**HQ1−33**, **HQ1−333**). The influence of the polyamine sequence on the selective uptake by the PTS in CHO cells was previously reported by using a collection (a set) of polyamine−anthracene conjugates.[28] Our results were in good agreement with this study showing the higher PTS selectivity of the 4,4-triamine analogues, its decrease after terminal amino-butylation such as in the 4,4,4-tetraamine and the lower PTS recognition of polyamine derivatives bearing a 3,3-triamine chain. In agreement with this previous study, 34 chains (**HQ1−34**, **HQ1−344**, **HQ1−343**) appeared to be poorly, or not, recognized by the PTS (Table 2). These similarities in the PTS targeting of our Quilamines and the polyamine−anthracene conjugates suggested the same cell uptake pathways for these two families of polyamine-analogues even if they could hit different cellular targets (DNA intercalation or iron depletion). The greater selectivity of the Quilamine **HQ1−44** for the PTS is in close agreement with previous works showing the higher cellular uptake of azepine−polyamine[31] and anthryl−polyamine[38] conjugates bearing a homospermidine chain.[44]

Complexation Properties of Quilamines toward Iron-(III) and Competitive Cations. *Comparison of the Chelation Efficiency of Quilamines **HQ1-XYZ**, 8-HQ, ICL670, and O-Trensox.* The cellular labile iron pool (LIP) consists of chelatable and redox-active iron, which plays a key role as a crossroads of cell iron metabolism. The ability of iron chelators to mobilize this temporary iron pool bound to low-molecular-weight and low-iron-affinity chelators (citrate, ascorbate, phosphate, and adenosine triphosphate) is an essential factor influencing their biological efficiency. According to previous work, the calcein test can predict the iron-chelating efficiency of chelators.[63,64] Thus, an acellular calcein test was performed to compare the potential ability of Quilamines **HQ1-*XYZ***, ICL670, O-Trensox, and 8-HQ, iron chelators used as references, to chelate this labile iron pool at physiological pH. In solution, calcein, a fluoresceinated analogue of EDTA, binds iron(II) and, more slowly, iron(III).[65] The fluorescence of this metallosensor dye is quenched during its interaction with iron and, conversely, is restored if iron is removed from the [calcein-Iron] complex by a most efficient competitive iron chelator. The rate and extent of fluorescence recovery depend on the chelator concentration, the kinetics and stoichiometry of iron binding and the relative binding affinity. The calcein test is qualitative, but the concentration of the chelator for which 50% of the fluorescence is restored is indicative of the chelator affinity (RC_{50}).

Recovered calcein fluorescence was measured in aqueous medium 30 min after the addition of the competitive chelators and is reported as a function of their concentrations in Figure 4. As expected from their relative affinity for iron(III), the three reference chelators, 8-HQ, ICL670, and O-Trensox, exhibited RC_{50} values equal to 4, 1.4, and 0.9 μM, respectively (Table 3). Curves of calcein fluorescence recovery were monophasic for the three reference chelators, while they showed two distinct components for all Quilamines. The first component (C1) was observed in the micromolar range of concentrations and the second one for Quilamine concentrations higher than 10 μM (C2). These biphasic curves were fitted as a double four-

dx.doi.org/10.1021/bc300324c | *Bioconjugate Chem.* 2012, 23, 1952−1968

Table 1. Cytostatic/Cytotoxic Effects and IC_{50} of Quilamines HQ1-*XYZ*, 8-HQ, and ICL670 in the CHO Cell Line

	% component 1 (*Cytostatic*)[a]	IC_{50}-1 (μM)	%LDH/control (10 μM)	% component 2 (*Cytotoxic*)[b]	IC_{50}-2 (μM)	%LDH/control (100 μM)
HQ1−44	80	1.2	102	20	11	125
HQ1−444	55	1.8	105	45	65	204
HQ1−443	35	1	100	65	45	203
HQ1−33	60	2	102	40	45	378
HQ1−333	0	ND	111	100	15	124
HQ1−43	0	ND	97	100	30	228
HQ1−34	30	20	111	70	110	200
HQ1−344	18	2	101	82	70	160
HQ1−343	0	ND[c]	93	100	27	199
8-HQ	0	ND[c]	259	100	4	245
ICL670	20	3	108	80	11	402

[a]Cytostatic effect was determined by measuring DNA content after Hoescht staining. Dose−effect curves were fitted as a double four-parameter fit to calculate the percentage of cells involved in each viability component (cytostatic and cytotoxic) as well as their corresponding IC_{50}. [b]Cytotoxic effect was evaluated by measuring LDH leakage into the culture medium. [c]ND, not detectable.

Table 2. Selectivity of Quilamines for the PTS. Effect of Quilamines HQ1-*XYZ*, 8-HQ, and ICL670 in CHO and CHO-MG Cells

	IC_{50} (μM)		IC_{50} ratio[a]
compounds	CHO	CHO-MG	CHO-MG/CHO
HQ1−44	1.4	344.5	249
HQ1−444	6.3	239.5	38
HQ1−443	20.2	257.5	13
HQ1−33	5.7	117.9	21
HQ1−333	15.1	277.0	18
HQ1−43	31.3	163.5	5
HQ1−34	93.1	152.0	2
HQ1−344	55.9	207.1	4
HQ1−343	27.0	105.7	4
8-HQ	5.0	6.5	1
ICL670	9.2	8.0	1

[a]This denotes the (CHO/CHO-MG) IC_{50} ratio, a measurement of PTS selectivity.

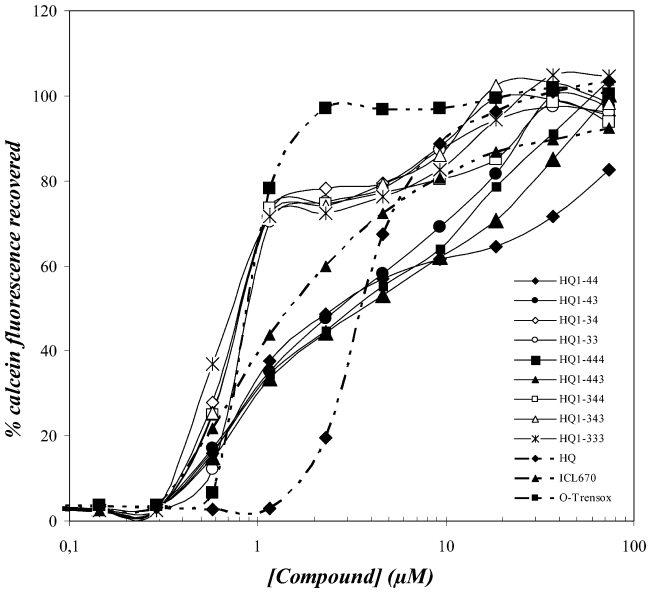

Figure 4. Comparison of the iron-chelating efficiency of Quilamines **HQ1-*XYZ*** with 8-HQ, ICL670, and O-Trensox, by calcein fluorescence measurements in a cell-free system.

Table 3. Percentage of Each Component and RC_{50} of HQ1-*XYZ*, 8-HQ, ICL670, and O-Trensox

compound	% component 1[a] (C1)	RC_{50}-1 (μM)	% component 2 (C2)	RC_{50}-2 (μM)
HQ1−44	58	1	42	57
HQ1−43	55	1	45	15
HQ1−444	53	1	47	18
HQ1−443	53	1	47	25
HQ1−34	78	0.7	22	10
HQ1−33	76	0.8	24	10
HQ1−344	74	0.65	26	20
HQ1−343	74	0.65	26	10
HQ1−333	72	0.6	28	12
8-HQ	100	4	0	0
ICL670	100	1.4	0	0
O-Trensox	100	0.9	0	0

[a]Biphasic curves (Figure 4) were fitted as a double four-parameter fit to calculate the percentage of each component as well as their corresponding concentration inducing half-fluorescence recovery (RC_{50}).

parameter fit to calculate the percentage of each component, as well as their corresponding concentration inducing half-fluorescence recovery (RC_{50}, Table 3). The first component C1 was greater with Quilamines **HQ1−3*YZ*** (72−78% with RC_{50} = 0.6−0.8 μM) than with Quilamines **HQ1−4*YZ*** (53−58% with RC_{50} = 1 μM). The ability of Quilamines to transchelate iron from calcein was between those of 8-hydroxyquinoline and O-Trensox. The shape of these curves (Figure 4) allowed two distinct groups of Quilamines to be discriminated: **HQ1−3*YZ*** (**HQ1−34**, **HQ1−33**, **HQ1−344**, **HQ1−343**, **HQ1−333**) and **HQ1−4*YZ*** (**HQ1−44**, **HQ1−43**, **HQ1−444**, **HQ1−443**) and suggested different modes of interaction with iron, probably modulated by the polyamine chain structure. Due to their amino groups, polyamines are able to chelate metallic cations.[66] The stability constants of these chelates increase with the number of amino groups and with the chain length of the polyamine.[67] Our results suggest the involvement of the amine group of the polyamine chain in the formation of iron complexes, as expected during the design and

synthesis of this Quilamine concept. The first secondary amine in Quilamines **HQ1** could be involved in iron coordination and probably the second one too, as deduced from the better iron-chelating efficiency of Quilamines **HQ1−3***YZ* compared to Quilamines **HQ1−4***YZ*.

*Complexation Properties of Quilamine **HQ1−44** toward Iron(III) and Competitive Cations.* To understand better the high iron affinity observed for the most promising chelator Quilamine **HQ1−44**, we assessed its complexation behavior toward iron(III) as well as other relevant cations such as copper(II), zinc(II), and magnesium(II), which may act as endogenous competitors of iron(III). This study was performed by potentiometric titrations in aqueous solutions at 25 °C. The ionic strength was adjusted to 0.10 M with potassium nitrate.

As a starting point, the acid−base properties of **HQ1−44** were first determined in the form of the protonation constants corresponding to its five basic centers located at the four amines and the single hydroxyl function. The calculated overall (log β) and stepwise (log K or pK_a) protonation constants are presented in Table 4. The four most basic centers were easily determined and have pK_a's in the range of 8−11, while the remaining center shows a much lower basicity with a pK_a that can just be estimated at around 1.3 as it is outside the accurate experimental range of the potentiometric technique used. The constants obtained can be understood in light of the known acid−base properties of the two functional moieties that constitute the ligand, 8-hydroxyquinoline[68] and homospermidine.[69] The highest pK_a of 10.83 must correspond to the protonation of the primary amine. The pK_a at 9.81 can easily be assigned to protonation of the hydroxyl group, as the yellow color of the ligand solution intensifies visibly around this pH value. The two remaining basic pK_a's of 9.05 and 7.98 belong to the two secondary amines, but it is not possible to assign the values individually. The acidic pK_a at 1.3 must be assigned to the protonation of the pyridine, as it is the least basic group in the chelator due to the close vicinity of the electron-withdrawing hydroxyl and secondary amine groups.

Table 4. Overall and Stepwise Protonation Constants for Compound HQ1-44 (25.0 °C, I = 0.10 M in KNO_3)

species[a]	log β	log K (pK_a)
HL	10.83	10.83
H_2L	20.64	9.81
H_3L	29.69	9.05
H_4L	37.67	7.98
H_5L	(39.0)[b]	(1.3)[b]

[a]HL = **HQ1−44**, and charges are omitted for the sake of clarity. [b]Values in brackets are approximate.

Next, we turned our attention to the complexation of iron(III). Since **HQ1−44** presents a total of 5 potential donor atoms for metal coordination, we performed potentiometric titrations with different amounts of metal in order to obtain a complete insight into the potential 1:2 and 1:1 metal-to-ligand complexation modes and the corresponding complex species. Thus, metal ratios of approximately 0.5 equiv and 1 equiv of iron(III) (relative to the ligand amount) were used during complexation titrations, and the titration curves obtained were used jointly to refine the complete model of stability constants for all the complex species. For both iron(III) ratios, species of 1:2 and 1:1 stoichiometry were present in equilibrium, with a predominance of 1:1 species for the higher amount of iron(III). There was an increasing tendency to form insoluble species above neutral pH, most likely hydroxocomplex species, with high amounts of iron(III). By refining together all the titrations performed, thermodynamic stability constants could be obtained accurately for only a limited set of complex species, mostly of 1:1 stoichiometry. This is due to some precipitation occurring at basic pH, which forced us to exclude the corresponding experimental results. However, as the amount of precipitate was small below pH = 9, we used the experimental data up to this pH in a separate refinement to obtain a rough approximation of the stability constants of the remaining species of 1:2 stoichiometry in order to gain an insight into the overall thermodynamic equilibria. A selection of calculated overall (log β) and stepwise (log K) stability constants is presented in Table 5 (a complete table showing the overall stability constants is available in ESI, Table S1).

Table 5. Overall and Stepwise Stability Constants for the Iron(III) Complexes of HQ1-44 (25.0 °C, I = 0.10 M in KNO_3)

species[a]	log β	log K
FeL	25.62	25.62
FeHL	32.13	6.51
FeH_2L	34.94	2.81
FeL_2	33.00	7.4
$FeHL_2$	42.20	9.2
FeH_2L_2	51.00	8.8
FeH_3L_2	59.10	8.1

[a]HL = **HQ1−44**, and charges are omitted for the sake of clarity.

Overall, we found that compound **HQ1−44** formed very strong iron(III) complexes. The thermodynamic stability of the complexes with 1:1 stoichiometry was very high, while that of complexes with 1:2 stoichiometry was more modest, as shown by the log K values of almost 26 for the former and below 8 for the latter. This clearly illustrates the preference of the ligand to form 1:1 complexes with adequate iron concentrations. However, the calculated overall log β values indicated that both 1:1 and 1:2 species were present successively in large amounts all along the pH scale: 1:1 species were formed between pH 2−6, while 1:2 species appeared above pH 6 with the largest amount occurring at around pH 7.5. This is demonstrated by the abundant presence of the three protonated species (log β around 60). This high thermodynamic stability also implies that a high complexation degree is attained at low pH values, with almost all of the iron(III) being chelated above pH = 3. This corresponds to a very small amount of free iron(III) present in solution at physiological pH (7.4), as indicated by a pFe^{3+} value of 19.4. It is thus clear that **HQ1−44** is a powerful chelator of iron(III).

We also studied the complexation of **HQ1−44** with competitive cations found *in vivo*. Titrations were performed in the presence of 0.5 equiv or 1 equiv of copper(II), and in the presence of 1 equiv of zinc(II) or magnesium(II). The calculated overall (log β) and stepwise (log K) stability constants are presented in Table S2 of the Supporting Information. The constant values show that strong complexes were formed with copper(II), with species of both 1:1 and 1:2 stoichiometries (pCu^{2+} = 12.6). The complexes of zinc(II) were only moderately stable, and also contained 1:1 and 1:2 species (pZn^{2+} = 7.8). With magnesium(II), only a few complex species of 1:1 stoichiometry were formed with an extremely low

stability (pMg^{2+} is insignificant). Distribution diagrams of the participating species for each metal are presented in ESI (SI Figures S2–S5). A competition diagram between Fe(III) and Zn(II) has been obtained from the values of all the stability constants with both metals; it clearly indicates the formation of a major amount of ternary species with Fe(III) all along the pH scale (in ESI SI Figure S6).

Taken together, these complexation studies prove that Quilamine **HQ1–44** forms very strong complexes with iron(III) and much weaker complexes with other endogenously relevant metal cations, indicative of a high selectivity for iron(III).

The preferential 1:2 [Fe/**HQ1–44**] stoichiometry of the ferric complex at pH = 7.4 was confirmed by the Job method of continuous variation (based on the MLCT (metal–ligand charge transfer) band) (Figure 5). The iron complex presents

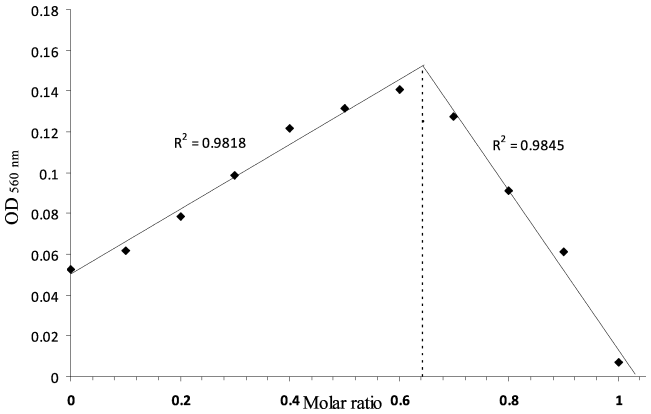

Figure 5. Job plot of **HQ1–44** at pH = 7.4 (λ_{max} = 560 nm). Solutions containing different ligand/Fe(III) ratios were prepared so that [ligand] + [Fe(III)] = 0.5 mM. The theoretical mole fraction maximum for a 2/1 ligand/Fe complex is 0.667; a linear intercept maximum of 0.65 was found.

colorimetric features (ε_{560} = 900 M^{-1} cm^{-1} for pH 7.4) and good stability properties (absorbance remains stable after several weeks). This clearly indicates that the homospermidine fragment of **HQ1–44** at pH = 7.4 alters the stoichiometry of the ferric complex. In fact, in the same conditions, hydroxyquinoline forms a 3:1 ligand/iron complex.

In view of this stoichiometry, it could be assumed that the iron complex [Fe/**HQ1–44**] forms three five-membered chelate rings in which the iron is probably coordinated by two vicinal *N*-atoms and a hydroxyl group (Figure 6). This

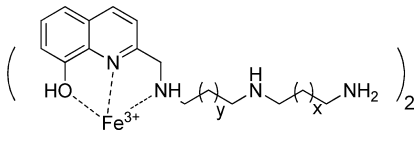

Figure 6. Hypothetical structure of **HQ1–44**/Fe complex with five-membered chelate rings.

stoichiometry was confirmed by elemental analysis, but unfortunately, repeated attempts to isolate X-ray quality crystals of the iron complex have so far been unsuccessful.

Due to the lack of the experimental electronic structure of metal complexes, the OPBE calculation was used to determine the energy and the structure of $[Fe\text{-}L_n]^{3+}$ (n = 1 or 2) complexes with a prototypical ligand **HQ1–1**.

Ab Initio Calculations. Density functional theory (DFT) calculations were carried out using the simplified model compound (**HQ1–1**) in which the polyamine moieties were replaced by a methylamine chain to render the calculations computationally tractable. All geometries reported in this paper are available in the Supporting Information. The ferric iron has 3d electrons and can thus adopt different spin configurations. The complexes were calculated in different spin states, but in all cases, the most stable Fe(III) complexes considered in this paper are high spin.

Despite the existence of a strong N_{qui}–HO hydrogen bond for the free ligand, which has been extensively studied by Shchavlev et al.,[70] iron(III) complexation is possible. The bonding in these complexes is expected to be dominated by ion–dipole electrostatic interactions although contributions arising from charge transfer, polarization, dispersion interactions, and exchange repulsive interactions at the equilibrium configuration of the complex are also likely to be present.

The geometries were compared with the bidentate ligand 8-HQ. The complexes were constructed by placing the ligands in pseudo-octahedral, but random, orientation about the metal under the C1 point group because we did not wish to presuppose any particular symmetry.

We modeled a highly stable complex like $[Fe(8\text{-}HQ)_n(H_2O)_{6-2n}]^{3+}$ (n = 1 or 2) to use as an energy reference and to consider reactions that correspond to an exchange of ligands (8-HQ and **HQ1–1**) as in eq 1.

$$[Fe(H_2O)_6]^{3+} + n\ 8\text{-HQ} \xrightleftharpoons{\beta_n(8\text{-HQ})} [Fe(8\text{-HQ})_n(H_2O)_{6-2n}]^{3+}$$
$$[Fe(H_2O)_6]^{3+} + n\ HQ1\text{-}1 \xrightleftharpoons{\beta_n(HQ1\text{-}1)} [Fe(HQ1\text{-}1)_n(H_2O)_{6-3n}]^{3+} \quad (1)$$
$$[Fe(8\text{-HQ})_n(H_2O)_{6-2n}]^{3+} + n\ HQ1\text{-}1 \xrightleftharpoons{K_n exc} [Fe(HQ1\text{-}1)_n(H_2O)_{6-3n}]^{3+} + n\ 8\text{-HQ} + n\ H_2O$$

The equilibrium constant of the exchange reactions can be calculated from the computed standard free energy change of reaction [1] *in vacuo*. All free energy values were negative, so the chelation reaction was highly exothermic (Table 6). On the basis of the log $K_n$exc obtained, the $[Fe(\mathbf{HQ1–1})_n(H_2O)_{6-3n}]^{3+}$ were the most stable for the 1:1 and 1:2 species.

The $[Fe(HQ1–1H)_2]^{5+}$ complex is not presented here because it leads to the formation of a tetrahedral complex, due to the repulsion of the protonated amines. Figure 7 shows the minimum energy structures obtained for $[Fe(8\text{-}HQ)_1(H_2O)_4]^{3+}$, $[Fe(8\text{-}HQ)_2(H_2O)_2]^{3+}$, $[Fe(HQ1–1)_1(H_2O)_3]^{3+}$, and $[Fe(HQ1–1)_2]^{3+}$ complexes. All are distorted octahedrons. The successive replacement of H_2O by the methylamine chain for **HQ1–1** results in an increase in both the average metal–ligand bond distance and the stabilization energy of the complex. The most stable structure for the $[Fe(HQ1–1)_2]^{3+}$ complex is a distorted octahedron in which oxygen and nitrogen atoms from both **HQ1–1** neutral ligands are bound to the metal. The symmetry of this complex is very close to the C2 symmetry. The two 8-hydroxyquinoline groups are planar and form a five-membered chelate ring with iron, leading to the facial monomer. The bond lengths with iron are in narrow ranges: between 2.084 and 2.190 Å for Fe(III)–N bonds and 2.474 Å for Fe(III)–O bonds. The Fe(III)–O distances are much longer than observed with $[Fe(H_2O)_6]^{3+}$: 1.995 Å.[71] The Fe(III)–N distances are also significantly longer than those observed in triazamacrocyclic complexes (i.e., 2.23–2.33 Å).[72] The average five-membered chelate ring (N_{qui}FeO

dx.doi.org/10.1021/bc300324c | *Bioconjugate Chem.* 2012, 23, 1952–1968

Table 6. Log β_n, Log $K_n$exc, Selected Bond Distances (Å) and Angles (deg) of Octahedral Complexes Determined by Quantum Chemical UOPBE/6-31G(d,p) and (Fe Lanl2DZ) Calculations

complex	$[Fe(8\text{-}HQ)_1(H_2O)_4]^{3+}$	$[Fe(\mathbf{HQ1-1})_1(H_2O)_3]^{3+}$	$[Fe(8\text{-}HQ)_2(H_2O)_2]^{3+}$	$[Fe(\mathbf{HQ1-1})_2]^{3+}$
Logβ_n	58	75	82	111
Log$K_n$exc		17		29
FeO_{qui}[a]	2.498	2.547	2.360 and 2.360	2.474 and 2.474
FeO_w[a]	2.145 and 2.176 and 2.176	2.131 and 2.200 and 2.243	2.200 and 2.200	
FeN_{qui}[a]	2.172	2.117	2.117 and 2.117	2.084 and 2.084
FeN_{ma}[a]		2.161		2.190 and 2.190
FeO_w[a]	2.146		2.200 and 2.200	
$N_{qi}FeO_{qui}$[a]	68.85	68.37	72.18 and 72.18	70.34 and 70.34
$N_{qi}FeN_{am}$[a]		78.82		78.21 and 78.21
$N_{qi}FeO_w$[a]	93.92 and 93.92 and 102.65 and 150.77	94.16 and 97.77 and 157.95	97.29 and 97.29 and 99.97 and 99.97	
$N_{qi}FeO_{qui}$[a]				146.10 and 146.10
$O_{qi}FeO_{qui}$[a]			92.79	82.40
$N_{qi}FeN_{qui}$[a]			155.85	163.19
$N_{ma}FeN_{ma}$[a]				114.42
O_wFeO_w[a]	88.01 and 88.01 and 87.14 and 87.14 and 106.57 and 171.82	83.62 and 84.31 and 167.77	88.38	

[a] N_{qui}: N of quinoline, N_{ma}: N of methylamine, O_{qui}: O of quinoline, O_w: O of water.

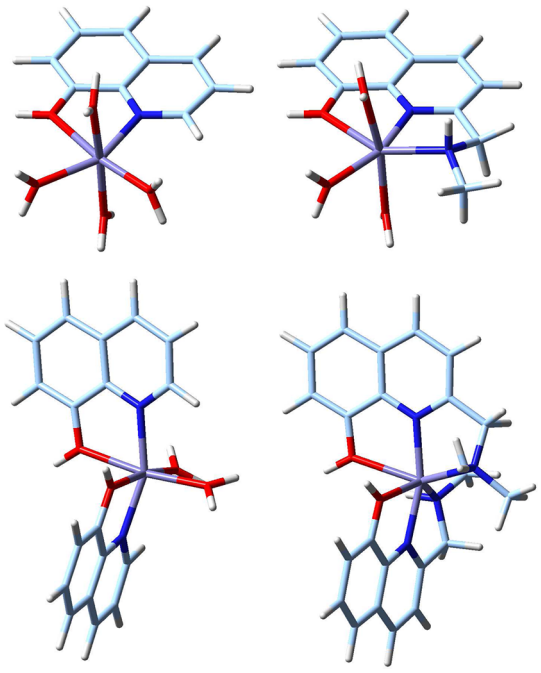

Figure 7. Minimum energy structures for $[Fe(8\text{-}HQ)_1(H_2O)_4]^{3+}$, $[Fe(\mathbf{HQ1-1})_1(H_2O)_3]^{3+}$, $[Fe(8\text{-}HQ)_2(H_2O)_2]^{3+}$, and $[Fe(\mathbf{HQ1-1})_2]^{3+}$ determined by quantum chemical UOPBE/6-31G(d,p) and (Fe Lanl2DZ) calculations.

and $N_{qui}FeN_{ma}$) is 74° (compared to 90° for an ideal octahedron). The apical angles ($N_{qui}FeO$ and $N_{ma}FeN_{ma}$) are 146.10°, 146.10°, and 163.19° (compared to 180° for an ideal octahedron). However, this distorted geometry does not impair the affinity of **HQ1−1** for iron as evidenced in the potentiometric assay.

CONCLUSION

We have developed a new type of iron chelator where an 8-hydroxyquinoline chelating subunit is grafted to polyamine vectors, in order to vectorize the iron chelator inside the cancerous cell with an overactive polyamine transport system (PTS). Nine Quilamines **HQ1-*XYZ***, differing in the nature of their polyamine chain, were synthesized in six or nine steps with good yields. The influence of the polyamine chain on the selective recognition of different Quilamines by the PTS was evidenced by comparing the antiproliferative activity obtained on a cell line displaying an efficient PTS (CHO) with that on a PTS-deficient mutant cell line (CHO-MG). This screening led us to choose the molecule **HQ1−44** from the synthesized Quilamines. The antiproliferative effect of **HQ1−44** occurred in the micromolar range, while a significant cytotoxicity was only observed at concentrations higher than 100 μM. We also demonstrated the high complexation capacity of **HQ1−44** with iron, while much weaker complexes were formed with other competitive cations. The ferric complex was shown to adopt preferentially a 1:2 [Fe/**HQ1−44**] stoichiometry at pH = 7.4. The binding energies and the equilibrium geometries of $[Fe\text{-}L_n]^{3+}$ (n = 1 or 2) complexes were assessed *in vacuo* from *ab initio* calculations. The stronger equilibrium constant of the exchange reactions between iron(III) and **HQ1−1** compared to 8-HQ was deduced from these calculations. The Quilamine is a tridentate ligand for iron(III) where both nitrogen and oxygen atoms form five-membered chelate rings.

In summary, Quilamines, and particularly **HQ1−44**, may be promising compounds for iron depletion in cancer therapies, due to their high affinity and selectivity for iron, their high antiproliferative activity associated with a low cytotoxicity, and their selective uptake by the PTS.

Further studies will evaluate the following: (i) the influence of modifying the length and the nature of the spacer between the chelating moiety and the homospermidine chain; (ii) the capacity to redox cycle and the generation of reactive oxygen species (ROS) (like the objective is an antitumor effect, the induction of oxidative stress may actually be a beneficial feature of an iron-chelator complex); (iii) the biological mechanisms of action of Quilamines, especially of **HQ1−44**; (iv) the antiproliferative efficiency of the Quilamine **HQ1−44** *in vitro* in various human tumor cell lines and *in vivo* in animal models.

dx.doi.org/10.1021/bc300324c | *Bioconjugate Chem.* 2012, 23, 1952−1968

■ ASSOCIATED CONTENT

Supporting Information

DFMO and exogenous spermidine treatments, stability constant data, and Cartesian coordinates of optimized structures. This material is available free of charge via the Internet at http://pubs.acs.org.

■ AUTHOR INFORMATION

Corresponding Author

* David Deniaud, Ph.D.: Phone 00-33-2-51125406, Fax 00-33-2-51125402, E-mail: david.deniaud@univ-nantes.fr. François Gaboriau, Ph.D.: Phone 00-33-2-23233861, Fax 00-33-2-99540137, E-mail: francois.gaboriau@univ-rennes1.fr.

Notes

The authors declare no competing financial interest.

■ ACKNOWLEDGMENTS

The authors are grateful to the Conseil Régional Pays de la Loire, to the French Ministry of Education, to the Ligue Nationale contre le Cancer (LNCC, Ille et Vilaine/Loire Atlantique), to the Association pour la Recherche sur le Cancer (ARC), and to the Centre National de la Recherche Scientifique (CNRS) for financial support. The geometry optimizations and the vibrational calculations reported in this paper were performed at CCIPL (Centre de Calcul Intensif des Pays de la Loire, Nantes, France) regional supercomputing center thanks to a dedicated CPU grant.

■ REFERENCES

(1) Richardson, D. R., Kalinowski, D. S., Lau, S., Jansson, P. J., and Lovejoy, D. B. (2009) Cancer cell iron metabolism and the development of potent iron chelators as anti-tumour agents. *Biochim. Biophys. Acta 1790*, 702−717.

(2) Kwok, J. C., and Richardson, D. R. (2002) The iron metabolism of neoplastic cells: alterations that facilitate proliferation? *Crit. Rev. Oncol. Hematol. 42*, 65−78.

(3) Brookes, M. J., Hughes, S., Turner, F. E., Reynolds, G., Sharma, N., Ismail, T., Berx, G., McKie, A. T., Hotchin, N., Anderson, G. J., Iqbal, T., and Tselepis, C. (2006) Modulation of iron transport proteins in human colorectal carcinogenesis. *Gut 55*, 1449−1460.

(4) Kolberg, M., Strand, K. R., Graff, P., and Andersson, K. K. (2004) Structure, function, and mechanism of ribonucleotide reductases. *Biochem. Biophys. Acta 1699*, 1−34.

(5) Ali, M. A., Akhmedkhanov, A., Zeleniuch-Jaquotte, A., Toniolo, P., Frenkel, K., and Huang, X. (2003) Reliability of serum iron, ferritin, nitrite, and association with risk of renal cancer in women. *Cancer Detect. Prev. 27*, 116−121.

(6) Huang, X. (2003) Iron overload and its association with cancer risk in humans: evidence for iron as a carcinogenic metal. *Mutat. Res. 533*, 153−171.

(7) Thompson, H. J., Kennedy, K., Witt, M., and Juzefyk, J. (1991) Effect of dietary iron deficiency or excess on the induction of mammary carcinogenenis by 1-methyl-1-nitrosourea. *Carcinogenesis 12*, 111−114.

(8) Daniels, T. R., Delgado, T., Rodriguez, J. A., Helguera, G., and Penichet, M. L. (2006) The transferrin receptor part I: Biology and targeting with cytotoxic antibodies for the treatment of cancer. *Clin. Immunol. 121*, 144−158.

(9) Pinnix, Z. K., Miller, L. D., Wang, W., D'Agostino, R., Jr., Kute, T., Willingham, M. C., Hatcher, H., Tesfay, L., Sui, G., Di, X., Torti, S. V., and Torti, F. M. (2010) Ferroportin and iron regulation in breast cancer progression and prognosis. *Sci. Transl. Med. 2*, 43−56.

(10) Pogribny, I. P. (2010) Ferroportin and hepcidin: a new hope in diagnosis, prognosis, and therapy for breast cancer. *Breast Cancer Res. 12*, 314−315.

(11) Richardson, D. R. (2002) Iron chelators as therapeutic agents for the treatment of cancer. *Crit. Rev. Oncol. Hematol. 42*, 267−281.

(12) Hoffbrand, A. V., Cohen, A., and Hershko, C. (2003) Role of deferiprone in chelation therapy for transfusional iron overload. *Blood*, 17−24.

(13) Maggio, A., D'Amico, G., Morabito, A., Capra, M., Ciaccio, C., Cianciulli, P., Di Gregorio, F., Garozzo, G., Malizia, R., Magnano, C., Mangiagli, A., Quarta, G., Rizzo, M., D'Ascola, D. G., Rizzo, A., and Midiri, M. (2002) Deferiprone versus deferoxamine in patients with thalassemia major: a randomized clinical trial. *Blood Cells, Molecules, and Diseases 28*, 196−208.

(14) Cappellini, M. D., Cohen, A., Piga, A., Bejaoui, M., Perrotta, S., Agaoglu, L., Aydinok, Y., Kattamis, A., Kilinc, Y., Porter, J., Capra, M., Galanello, R., Fattoum, S., Drelichman, G., Magnano, C., Verissimo, M., Athanassiou-Metaxa, M., Giardina, P., Kourakli-Symeonidis, A., Janka-Schaub, G., Coates, T., Vermylen, C., Olivieri, N., Thuret, I., Opitz, H., Ressayre-Djaffer, C., Marks, P., and Alberti, D. (2006) A phase 3 study of deferasirox (ICL670), a once-daily oral iron chelator, in patients with beta-thalassemia. *Blood 107*, 3455−3462.

(15) Chantrel-Groussard, K., Gaboriau, F., Pasdeloup, N., Havouis, R., Nick, H., Pierre, J. L., Brissot, P., and Lescoat, G. (2006) The new orally active iron chelator ICL670A exhibits a higher antiproliferative effect in human hepatocyte cultures than O-trensox. *Eur. J. Pharmacol. 541*, 129−137.

(16) Gaboriau, F., Laupen-Chassay, C., Pasdeloup, N., Pierre, J.-L., Brissot, P., and Lescoat, G. (2006) Modulation of cell proliferation and polyamine metabolism in rat liver cell cultures by the iron chelator O-trensox. *BioMetals 19*, 623−632.

(17) Richardson, D., Ponka, P., and Baker, E. (1994) The effect of the iron(III) chelator, desferrioxamine, on iron and transferrin uptake by the human malignant melanoma cell. *Cancer Res. 54*, 685−9.

(18) Donfrancesco, A., Deb, G., De Sio, L., Cozza, R., and Castellano, A. (1996) Role of deferoxamine in tumor therapy. *Acta Haematol. 95*, 66−69.

(19) Saletta, F., Rahmanto, Y. S., Siafakas, A. R., and Richardson, D. R. (2011) Cellular iron depletion and the mechanisms involved in the iron-dependent regulation of the growth arrest and DNA damage family of genes. *J. Biol. Chem. 286*, 35396−35406.

(20) Wallace, H. M., Fraser, A. V., and Hughes, A. (2003) A perspective of polyamine metabolism. *Biochem. J. 376*, 1−14.

(21) Grillo, M. A., and Colombatto, S. (1994) Polyamine transport in cells. *Biochem. Soc. Trans. 22*, 894−898.

(22) Palmer, A. J., and Wallace, H. M. (2010) The polyamine transport system as a target for anticancer drug development. *Amino Acids 38*, 415−422.

(23) Seiler, N. (2003) Thirty years of polyamine-related approaches to cancer therapy. Retrospect and prospect. Part 2. Structural analogues and derivatives. *Curr. Drug Targets 4*, 565−585.

(24) Seiler, N. (2003) Thirty years of polyamine-related approaches to cancer therapy. Retrospect and prospect. Part 1. Selective enzyme inhibitors. *Curr. Drug Targets 4*, 537−564.

(25) Holley, J., Mather, A., Cullis, P., Symons, M. R., Wardman, P., Watt, R. A., and Cohen, G. M. (1992) Uptake and cytotoxicity of novel nitroimidazole-polyamine conjugates in Ehrlich ascites tumour cells. *Biochem. Pharmacol. 43*, 763−769.

(26) Verschoyle, R. D., Carthew, P., Holley, J. L., Cullis, P., and Cohen, G. M. (1994) The comparative toxicity of chlorambucil and chlorambucil-spermidine conjugate to BALB/c mice. *Cancer Lett. 85*, 217−222.

(27) Delcros, J. G., Tomasi, S., Carrington, S., Martin, B., Renault, J., Blagbrough, I. S., and Uriac, P. (2002) Effect of spermine conjugation on the cytotoxicity and cellular transport of acridine. *J. Med. Chem. 45*, 5098−5111.

(28) Phanstiel, O., IV, Kaur, N., and Delcros, J. G. (2007) Structure-activity investigations of polyamine-anthracene conjugates and their uptake via the polyamine transporter. *Amino Acids 33*, 305−313.

(29) Dallavalle, S., Giannini, G., Alloatti, D., Casati, A., Marastoni, E., Musso, L., Merlini, L., Morini, G., Penco, S., Pisano, C., Tinelli, S., De Cesare, M., Beretta, G. L., and Zunino, F. (2006) Synthesis and

cytotoxic activity of polyamine analogues of camptothecin. *J. Med. Chem. 49*, 5177−86.
(30) Esteves-Souza, A., Lucio, K. A., Da Cunha, A. S., Da Cunha Pinto, A., Da Silva Lima, E. L., Camara, C. A., Vargas, M. D., and Gattass, C. R. (2008) Antitumoral activity of new polyamine-naphthoquinone conjugates. *Oncol. Rep. 20*, 225−231.
(31) Tomasi, S., Renault, J., Martin, B., Duhieu, S., Cerec, V., Le Roch, M., Uriac, P., and Delcros, J. G. (2010) Targeting the polyamine transport system with benzazepine- and azepine-polyamine conjugates. *J. Med. Chem. 53*, 7647−7663.
(32) Burns, M. R., Graminski, G. F., Weeks, R. S., Chen, Y., and O'Brien, T. G. (2009) Lipophilic lysine-spermine conjugates are potent polyamine transport inhibitors for use in combination with a polyamine biosynthesis inhibitor. *J. Med. Chem. 52*, 1983−1993.
(33) Covassin, L., Desjardins, M., Soulet, D., Charest-Gaudreault, R., Audette, M., and Poulin, R. (2003) Xylylated dimers of putrescine and polyamines: influence of the polyamine backbone on spermidine transport inhibition. *Bioorg. Med. Chem. Lett. 13*, 3267−3271.
(34) Delcros, J. G., Vaultier, M., Roch, N. L., Havouis, R., Moulinoux, J. P., and Seiler, N. (1997) Bis(7-amino-4-azaheptyl)dimethylsilane: a new tetramine with polyamine-like features. Effects on cell growth. *Anti-cancer Drug Design 12*, 35−48.
(35) Martin, B., Posseme, F., Le Barbier, C., Carreaux, F., Carboni, B., Seiler, N., Moulinoux, J. P., and Delcros, J. G. (2002) Z)-1,4-diamino-2-butene as a vector of boron, fluorine, or iodine for cancer therapy and imaging: synthesis and biological evaluation. *Bioorg. Med. Chem. 10*, 2863−2871.
(36) Zhuo, J. C., Cai, J., Soloway, A. H., Barth, R. F., Adams, D. M., Ji, W., and Tjarks, W. (1999) Synthesis and biological evaluation of boron-containing polyamines as potential agents for neutron capture therapy of brian tumors. *J. Med. Chem. 42*, 1282−1292.
(37) Annereau, J. P., Brel, V., Dumontet, C., Guminski, Y., Imbert, T., Broussas, M., Vispe, S., Breand, S., Guilbaud, N., Barret, J. M., and Bailly, C. (2010) A fluorescent biomarker of the polyamine transport system to select patients with AML for F14512 treatment. *Leuk. Res. 34*, 1383−1389.
(38) Wang, C., Delcros, J. G., Biggerstaff, J., and Phanstiel, O., IV (2003) Synthesis and biological evaluation of N1-(anthracen-9-ylmethyl)triamines as molecular recognition elements for the polyamine transporter. *J. Med. Chem. 46*, 2663−2671.
(39) Wang, C., Delcros, J.-G., Biggerstaff, J., and Phanstiel, O., IV (2003) Molecular requirements for targeting the polyamine transport system. synthesis and biological evaluation of polyamine anthracene conjugates. *J. Med. Chem. 46*, 2672−2682.
(40) Kruczynski, A., Vandenberghe, I., Pillon, A., Pesnel, S., Goetsch, L., Barret, J. M., Guminski, Y., Le Pape, A., Imbert, T., Bailly, C., and Guilbaud, N. (2011) Preclinical activity of F14512, designed to target tumors expressing an active polyamine transport system. *Invest. New Drugs 29*, 9−21.
(41) Bergeron, R. J., Singh, S., Bharti, N., and Jiang, Y. (2010) Design, synthesis, and testing of polyamine vectored iron chelators. *Synthesis*, 3631−3636.
(42) Baret, P., Béguin, C. G., Boukhalfa, H., Caris, C., Laulhere, J. P., Pierre, J. L., and Serratrice, G. (1995) O-TRENSOX: A promizing water-soluble iron chelator (both FeIII and FeII) potentially suitable for plant nutrition and iron chelation therapy. *J. Am. Chem. Soc. 117*, 9760−9761.
(43) Du, T., Filiz, G., Caragounis, A., Crouch, P. J., and White, A. R. (2008) Clioquinol promotes cancer cell toxicity through tumor necrosis factor alpha release from macrophages. *J. Pharmacol. Exp. Ther. 324*, 360−367.
(44) Ding, W. Q., Liu, B., Vaught, J. L., Palmiter, R. D., and Lind, S. E. (2006) Clioquinol and docosahexaenoic acid act synergistically to kill tumor cells. *Mol. Cancer Ther. 5*, 1864−1872.
(45) Wang, J., Xie, S., Li, Y., Guo, Y., Ma, Y., Zhao, J., Phanstiel, O., IV, and Wang, C. (2008) Synthesis and evaluation of unsymmetrical polyamine derivatives as antitumor agents. *Bioorg. Med. Chem. 16*, 7005−7012.
(46) Byers, T. L., and Pegg, A. E. (1989) Properties and physiological function of the polyamine transport system. *Am. J. Physiol. 257* (Cell. physiol. 26), C545−C553.
(47) Rodbard, D., and McClean, S. W. (1977) Automated computer analysis for enzyme-multiplied immunological techniques. *Clin. Chem. 23*, 112−115.
(48) Swart, M., Groenhof, A. R., Ehlers, A. W., and Lammertsma, K. (2004) Validation of exchange-correlation functionals for spin states of iron complexes. *J. Phys. Chem. A 25*, 5479−5483.
(49) Handy, A. J., and Cohen, N. C. (2001) Left-right correlation energy. *Mol. Phys.*, 403−412.
(50) Perdew, J. P., Burke, K., and M., E. (1997) Generalized gradient approximation made simple [phys. rev. lett. 77, 3865 (1996)]. *Phys. Rev. Lett. 7*, 1396−1398.
(51) Frisch, M. J., Trucks, G. W., Schlegel, H. B., Scuseria, G. E., Robb, M. A., Cheeseman, J. R., Scalmani, G., Barone, V., Mennucci, B., Petersson, G. A., Nakatsuji, H., Caricato, M., Li, X., Hratchian, H. P., Izmaylov, A. F., Bloino, J., Zheng, G., Sonnenberg, J. L., Hada, M., Ehara, M., Toyota, K., Fukuda, R., Hasegawa, J., Ishida, M., Nakajima, T., Honda, Y., Kitao, O., Nakai, H., Vreven, T., Montgomery, J., J. A., Peralta, J. E., Ogliaro, F., Bearpark, M., Heyd, J. J., Brothers, E., Kudin, K. N., Staroverov, V. N., Kobayashi, R., Normand, J., Raghavachari, K., Rendell, A., Burant, J. C., Iyengar, S. S., Tomasi, J., Cossi, M., Rega, N., Millam, J. M., Klene, M., Knox, J. E., Cross, J. B., Bakken, V., Adamo, C., Jaramillo, J., Gomperts, R., Stratmann, R. E., Yazyev, O., Austin, A. J., Cammi, R., Pomelli, C., Ochterski, J. W., Martin, R. L., Morokuma, K., Zakrzewski, V. G., Voth, G. A., Salvador, P., Dannenberg, J. J., Dapprich, S., Daniels, A. D., Farkas, O., Foresman, J. B., Ortiz, J. V., Cioslowski, J., and J., F. D. (2009) *Gaussian 09 Revision A.02*, Gaussian Inc., Wallingford, CT.
(52) Kuksa, V., Buchan, R., and Kong Thoo Lin, P. (2000) Synthesis of polyamines, their derivatives, analogues and conjugates. *Synthesis*, 1189−1207.
(53) Tian, Z.-y., Xie, S.-q., Mei, Z.-h., Zhao, J., Gao, W.-y., and Wang, C.-j. (2009) Conjugation of substituted naphthalimides to polyamines as cytotoxic agents targeting the Akt/mTOR signal pathway. *Org. Biomol. Chem. 7*, 4651−4660.
(54) Bergeron, R. J., Bharti, N., Wiegand, J., McManis, J. S., Yao, H., and Prokai, L. (2005) Polyamine-vectored iron chelators: the role of charge. *J. Med. Chem. 48*, 4120−4137.
(55) Kaur, N., Delcros, J.-G., Archer, J., Weagraff, N. Z., Martin, B. n. d., and Phanstiel, O., Iv (2008) Designing the polyamine pharmacophore: influence of N-substituents on the transport behavior of polyamine conjugates. *J. Med. Chem. 51*, 2551−2560.
(56) Gardner, R. A., Belting, M., Svensson, K., and Phanstiel. (2007) Synthesis and transfection efficiencies of new lipophilic polyamines. *J. Med. Chem. 50*, 308−318.
(57) Xie, S., Cheng, P., Liu, G., Ma, Y., Zhao, J., Chehtane, M., Khaled, A. R., Phanstiel, Iv, O., and Wang, C. (2007) Synthesis and bioevaluation of N-(arylalkyl)-homospermidine conjugates. *Bioorg. Med. Chem. Lett. 17*, 4471−4475.
(58) Chadwick, J., Jones, M., Mercer, A. E., Stocks, P. A., Ward, S. A., Park, B. K., and O'Neill, P. M. (2010) Design, synthesis and antimalarial/anticancer evaluation of spermidine linked artemisinin conjugates designed to exploit polyamine transporters in Plasmodium falciparum and HL-60 cancer cell lines. *Bioorg. Med. Chem. 18*, 2586−2597.
(59) de Medina, P., Paillasse, M. R., Payre, B., Silvente-Poirot, S., and Poirot, M. (2009) Synthesis of new alkylaminooxysterols with potent cell differentiating activities: identification of leads for the treatment of cancer and neurodegenerative diseases. *J. Med. Chem. 52*, 7765−7777.
(60) Jotterand, N., Pearce, D. A., and Imperiali, B. (2001) Asymmetric synthesis of a new 8-hydroxyquinoline-derived alpha-amino acid and its incorporation in a peptidylsensor for divalent zinc. *J. Org. Chem. 66*, 3224−3228.
(61) Abdel-Magid, A. F., Carson, K. G., Harris, B. D., Maryanoff, C. A., and Shah, R. D. (1996) Reductive amination of aldehydes and ketones with sodium triacetoxyborohydride. studies on direct and indirect reductive amination procedures. *J. Org. Chem. 61*, 3849−3862.

(62) Byers, T. L., Wechter, R., Nuttall, M. E., and Pegg, A. E. (1989) Expression of a human gene for polyamine transport in Chinese-hamster ovary cells. *Biochem. J. 263*, 745−752.
(63) Lescoat, G., Léonce, S., Pierré, A., Gouffier, L., and Gaboriau, F. (2012) Antiproliferative and iron chelating efficiency of the new bis-8-hydroxyquinoline benzylamine chelator S1 in hepatocyte cultures. *Chem.-Biol. Interact. 195*, 165−172.
(64) Rodriguez-Lucena, D., Gaboriau, F., Rivault, F., Schalk, I. J., Lescoat, G., and Mislin, G. L. A. (2010) Synthesis and biological properties of iron chelators based on a bis-2-(2-hydroxy-phenyl)-thiazole-4-carboxamide or -thiocarboxamide (BHPTC) scaffold. *Bioorg. Med. Chem. 18*, 689−695.
(65) Thomas, F., Serratrice, G., Béguin, C., Saint Aman, E., Pierre, J. L., Fontecave, M., and Laulhère, J. P. (1999) Calcein as a fluorescent probe for ferric iron. *J. Biol. Chem. 274*, 13375−13383.
(66) Lovaas, E. (1997) Antioxidative and metal-chelating effects of polyamines. *Adv. Pharmacol.*, 119−149.
(67) Palmer, B. N., and Powell, H. K. J. (1974) Polyamine complexes with seven-membered chelate rings: Complexe formation of 3-azaheptane-1,7-diamine, 4-azaoctane-1,8-diamine (spermidine), and 4,9-diazadodecane-1,12-diamine (spermine) with copper(II) and hydrogen ions in aqueous solution. *J. Chem. Soc., Dalton Trans.*, 2089−2092.
(68) Bardez, E., Devol, I., Larrey, B., and Valeur, B. (1997) Excited-state processes in 8-hydroxyquinoline: photoinduced tautomerization and solvation effects. *J. Phys. Chem. B 101*, 7786−7793.
(69) Kimberly, M. M., and Goldstein, J. H. (1981) Determination of pKa values and total proton distribution pattern of spermidine by carbon-13 nuclear magnetic resonance titrations. *Anal. Chem. 53*, 789−793.
(70) Shchavlev, A. E., Pankratov, A. N., and Shalabay, A. V. (2006) Dft computational studies on rotation barriers, tautomerism, intramolecular hydrogen bond, and solvent effects in 8-hydroxyquinoline. *Int. J. Quantum Chem. 4*, 876−886.
(71) Beattie, J. K., Best, S. P., Skelton, B. W., and White, A. H. (1981) Structural studies on the caesium alums, $CsMIII[SO_4]_2 \bullet 12H_2O$. *J. Chem. Soc., Dalton Trans.*, 2105−2111.
(72) Notni, J., Pohle, K., Peters, J. A., Görls, H., and Platas-Iglesias, C. (2009) Structural study of Ga(III), In(III), and Fe(III) complexes of triaza-macrocycle based ligands with N3S3 donor set. *Inorg. Chem. 7*, 3257−3267.